Neural substrates of saccadic adaptation: plastic changes versus error processing and forward versus backward learning

Camille Métais, Judith Nicolas, Moussa Diarra, Alexis Cheviet, Eric Koun, Denis Pélisson

Title: Neural substrates of saccadic adaptation: plastic changes versus error processing and forward versus backward learning.

Short title: Brain functional activations during saccadic adaptation

Authors: Camille Métais[a], Judith Nicolas[a,b], Moussa Diarra[a,c], Alexis Cheviet[a], Eric Koun[a], Denis Pélisson[a]*

[a]IMPACT Team, Lyon Neuroscience Research Center, INSERM U1028; CNRS UMR5292; University Claude Bernard Lyon 1; 16, av. du Doyen Lépine, 69676 Bron cedex, France

[b]Present Address: Department of Movement Sciences, Movement Control and Neuroplasticity Research Group, KU Leuven, 3001 Leuven, Belgium

[c]Present Address: Université Bourgogne Franche-Comté, LEAD - CNRS UMR5022, Université de Bourgogne, Pôle AAFE, 11 Esplanade Erasme, 21000 Dijon, France.

*Corresponding author

Abstract:

Previous behavioral, clinical, and neuroimaging studies suggest that the neural substrates of adaptation of saccadic eye movements involve, beyond the central role of the cerebellum, several, still incompletely determined, cortical areas. Furthermore, no neuroimaging study has yet tackled the differences between saccade lengthening ("forward adaptation") and shortening ("backward adaptation") and neither between their two main components, i.e. error processing and oculomotor changes.

The present fMRI study was designed to fill these gaps. Blood-oxygen-level-dependent (BOLD) signal and eye movements of 24 healthy volunteers were acquired while performing reactive saccades under 4 conditions repeated in short blocks of 16 trials: systematic target jump during the saccade and in the saccade direction (forward: FW) or in the opposite direction (backward: BW), randomly directed FW or BW target jump during the saccade (random: RND) and no intra-saccadic target jump (stationary: STA). BOLD signals were analyzed both through general linear model (GLM) approaches applied at the whole-brain level and through sensitive Multi-Variate Pattern Analyses (MVPA) applied to 34 regions of interest (ROIs) identified from independent 'Saccade Localizer' functional data.

Oculomotor data were consistent with successful induction of forward and backward adaptation in FW and BW blocks, respectively. The different analyses of voxel activation patterns (MVPAs) disclosed the involvement of 1) a set of ROIs specifically related to adaptation in the right occipital cortex, right and left MT/MST, right FEF and right pallidum; 2) several ROIs specifically involved in error signal processing in the left occipital cortex, left PEF, left precuneus, Medial Cingulate cortex (MCC), left inferior and right superior cerebellum; 3) ROIs specific to the direction of adaptation in the occipital cortex and MT/MST (left and right hemispheres for FW and BW, respectively) and in the pallidum of the right hemisphere (FW). The involvement of the left PEF and of the (left and right) occipital cortex were further supported and qualified by the whole brain GLM analysis: clusters of increased activity were found in PEF for the RND versus STA contrast (related to error processing) and in the left (right) occipital cortex for the FW (BW) versus STA contrasts [related to the FW (BW) direction of error and/or adaptation].

The present study both adds complementary data to the growing literature supporting a role of the cerebral cortex in saccadic adaptation through feedback and feedforward relationships with the cerebellum and provides the basis for improving conceptual frameworks of oculomotor plasticity and of its link with spatial cognition.

Key Words (6 max): eye movements, target jumps, oculomotor error, sensorimotor adaptation, neural plasticity, fMRI

Highlights: (3 to 5 bullet points, maximum 85 characters, including spaces, per bullet point):

- Cortical substrates of saccadic plasticity and error processing are still unknown
- Our fMRI study shows substrates specific to plasticity processes & error processing
- Distinct neural substrates are also found for the two directions of adaptation
- Findings emphasize the link between saccadic plasticity and spatial cognition

1. INTRODUCTION

Exploration of our visual environment relies on the generation of saccadic eye movements about three times per second. Saccades are usually defined as “reactive” when reflexively triggered by sudden changes in the visual scene and as “voluntary” when intentionally elicited to explore a stable visual scene. Keeping saccades accurate despite life perturbations (like fatigue, aging, growth, neurological condition, etc) is therefore essential for our daily activities. This is achieved by saccadic adaptation. In the lab, this well-studied sensory-motor plasticity is induced with the double-step paradigm first described by McLaughlin (1967). This procedure consists in presenting a visual target that the participant is instructed to gaze at, and then in slightly shifting this target as soon as the saccade is launched. Going unnoticed due to saccadic suppression (Bridgeman et al., 1975), this intrasaccadic target displacement elicits an error signal which shortly triggers a secondary, corrective, saccade. When repeated in similar double-step trials (~100-200 in humans: Pélisson et al 2010), such error signals lead the saccadic system to progressively adapt and eventually aim closer to the displaced than to the initial target location. “Backward“ saccadic adaptation decreases saccade amplitude due to target shifts directed opposite to the saccade whereas “forward“ saccadic adaptation increases saccade amplitude in response to target shifts along the saccade direction.

An abundant literature has notably provided evidence that backward and forward saccadic adaptation involve different mechanisms. Indeed, it is a typical observation that, relative to backward adaptation, forward adaptation reaches a lower and more variable steady state level, which nonetheless requires more trials (e.g. Straube & Deubel, 1995, Ethier et al., 2008, Bey et al, 2021; for review Pélisson et al., 2010). Different changes of saccade dynamics (duration or peak velocity) between the two types of adaptation have also been observed in some studies (Golla et al., 2008; Schnier & Lappe, 2011). Importantly, the two types of adaptation seem to rely on different

substrates in the cerebellum, as shown by the opposite effects on backward adaptation (inhibition) and forward adaptation (boost) of trans-cranial magnetic stimulation (TMS) applied over the lateral cerebellar hemisphere (Crus I) (Panouillères et al., 2012a). Also, spatial patterns of adaptation transfer, i.e. from an adapted saccade originating at a given orbital position toward untrained saccades originating at varying orbital eye positions, can also differ between the two adaptation types, leading Semmlow et al. (1989) to suggest that forward adaptation involves target remapping processes whereas backward adaptation involves motor execution processes (see also Ethier et al., 2008). Furthermore, other studies showed that the two types of adaptation also differ in their pattern of transfer to other motor tasks, such as antisaccades (Panouillères et al., 2009), subsequent saccades in sequential tasks (Panouillères et al., 2012b) or hand pointing movements (Cotti et al., 2007: backward; Hernandez et al., 2008: forward). In these last studies, stronger transfers were observed following forward adaptation than after backward adaptation.

It has become clear over the last two decades that beyond motor changes, saccadic adaptation can also affect visuo-spatial localization and even attention (reviewed by Zimmermann & Lappe, 2016). Using localization tasks in the context of saccadic adaptation is particularly interesting since these tasks allow us to access the internal representations of the target and of the saccade itself, derived from the 'corollary discharge' (CD) of the oculomotor command, by contrasting fixation and trans-saccadic conditions, respectively (Cheviet et al., 2021). Moreover, saccadic adaptation can affect both kinds of internal representations as supported by recent modelling work (Masselink & Lappe, 2021). Indeed perceptual judgements of a flashed stimulus under gaze fixation became biased in the direction of the target shift after -versus before- a saccadic adaptation training phase, especially in the case of forward adaptation (Zimmermann & Lappe, 2010, 2011; Schnier & Lappe, 2012; Schnier et al., 2010; and in monkey: Gremmler et al., 2014), pleading in favour of Semmlow et al. (1989)'s remapping hypothesis. Additionally, an even stronger bias has been commonly observed when localization performance was assessed under a trans-saccadic condition (Bahcall & Kowler, 1999; Collins, Rolfs, Deubel & Cavanagh, 2009, Collins, Heed & Röder, 2010; Schnier, Zimmermann & Lappe, 2010; Klingenhoefer & Bremmer, 2011; Schnier & Lappe, 2012; Souto, Gegenfurtner & Schütz, 2016). Such perceptual biases observed in both gaze fixation and trans-saccadic conditions are consistent with the hypothesis that saccadic adaptation is a multicomponent plasticity process altering to different extents the motor command, its internal representation and the target internal representation (Masselink & Lappe, 2021; Cheviet et al., 2022). Finally, studies have disclosed that saccadic adaptation can modify the focus of visuospatial attention. This has been shown by the post-adaptation performance changes of the detection or discrimination of a visual stimulus presented either just before the saccadic response ('pre-saccadic' shift of attention: Doré-Mazars & Collins,

2005; Collins & Doré-Mazars, 2006; Khan et al., 2010) or under complete ocular fixation condition ('covert' shift of attention: Habchi et al., 2015; Nicolas et al., 2019a, 2020). Taken together, these studies of transfer to visuo-spatial perceptual tasks suggest that the neural substrates of saccadic adaptation may not be limited to oculomotor structures regulating the saccade amplitude, like the cerebellum and brainstem, but could additionally recruit cortical areas involved in visuo-spatial processing. Does this prediction match the state of current knowledge?

There is a large consensus on the critical involvement in saccadic adaptation of the cerebellum, both in humans (Desmurget et al., 1998, 2000; Straube et al., 2001; Alahyane et al., 2008; Choi et al., 2008; Golla et al., 2008; Xu-Wilson et al., 2009; Jenkinson & Miall, 2010; Panouillères et al., 2012a, 2013, 2015; Avila et al., 2015) and non-human primates (Optican & Robinson, 1980; Straube et al., 1997; Barash et al., 1999; Takagi et al., 1998). Among the human studies of adaptation neural substrates, only three used fMRI, as far as we know. All three focussed on backward adaptation of reactive saccades but nonetheless reported an involvement of the cerebral cortex: the supplementary eye fields (SEF) and the temporal lobe / posterior insula complex (Blurton et al., 2012); the temporo-parietal junction (TPJ), hMT/V5 complex, and a pre-frontal area corresponding to the frontal eye fields (FEF) (Gerardin et al., 2012); and the precuneus (Guillaume et al., 2018). Note that two additional areas of the intra-parietal sulcus (medial and posterior) were related to adaptation of voluntary saccades (Gerardin et al., 2012). Besides, patient studies have suggested that the cerebello-thalamo-cortical pathway plays a role in saccadic adaptation (Gaymard et al., 2001; Zimmerman et al., 2015). All together, these data suggest that the cerebellum is the core of a saccade adaptation neural system which also involves cortical areas. However, the role and exact extent of this cortical network is still unknown. In monkeys, a direct involvement of the cerebellum in computing and providing the brainstem saccade generator with an adaptation-related corrective signal is largely supported by physiological evidence (see Iwamoto and Kaku, 2010 for review); in contrast, a role of the cerebral cortex in saccadic adaptation has rarely been studied and remains disputed (e.g. Steenrod et al., 2013, but see Zhou et al., 2016). One possibility is that cortical areas subtend the saccade-related changes of visual perception which have been evidenced by the human behavioural studies reviewed above. According to this hypothesis, the changes of activity in the cerebral cortex, possibly through the influence of the cerebellum, would account for the perceptual effects of adaptation (Zimmerman et al., 2016). An alternative possibility is that the cerebral cortex is causally involved in adaptation, namely by contributing to the error processing mechanisms which trigger the adaptive oculomotor changes within the brainstem and cerebellum (Zhou et al., 2016; Guillaume et al., 2018). Note that in this second possibility, the cerebellum could also contribute to

such error processing function (Liem et al., 2012), simultaneously to its causal role in plastic oculomotor changes.

Thus, to overcome the limitations of knowledge delineated above, the first objective of the present fMRI study was to determine the cortical and subcortical areas involved in reactive saccade adaptation, as well as those specifically involved in encoding the visual error signal. Its second objective was to disclose any difference between the neural substrates involved in forward adaptation and in backward adaptation. This study implements a well-established target double-step procedure to compare forward and backward saccadic adaptations to each other, as well as to two non-adaptation conditions with or without a random error signal.

2. MATERIALS AND METHODS

2.1. Subjects

Twenty-four subjects participated in the experiment (13 females, mean age ± Standard Deviation – SD: 26 ± 4 years). All of them had a normal or corrected to normal vision, and none of them had any history of brain lesion or neurological disorder. Participants were instructed to restrain from alcohol and psychotropic substances consumption the day before the experiment and to have a good night of sleep. They gave their written informed consent and received a payment for their participation. All procedures fulfilled the Declaration of Helsinki's requirements and were approved by the ethics committee (CPP Est-III, France, ID-RCB: 2018-A00932-53).

2.2. Set-up and eye-movement recording

The experiment was performed with a 3-Tesla Siemens PRISMA MRI scanner (Siemens AG, Germany) at CERMEP (Centre d'Etude et de Recherche Multimodal Et Pluridisciplinaire, Bron, France). Participants' head was stabilised with foam padding and horizontal and vertical movements of the right eye were continuously recorded thanks to an EyeLink 1000 Plus infrared camera (SR Research, Canada), with a sampling rate of 1000 Hz (Illuminator: λ = 940 nm; spatial resolution = 0.01° (RMS); accuracy = 0.25-0.5°). Both infrared eye camera and illuminator were placed behind the scanner magnet, just outside the bore. A tilted mirror affixed to the head coil above the subjects' head permitted to transmit the image of the subjects' right eye to the Eyelink camera. The standard EyeLink calibration procedure was performed at the beginning of the session, before starting any scan acquisition, using the following 5 points: 1 central point (0°/0°), 1 point above (0°/+10.1°), 1 point below (0°/-10.1°), 1 point left (-18°/0°) and 1 point right (+18°/0°).

The computer image (screen resolution: 1920*1080; refresh rate: 120 Hz) was projected through a VPixx projector onto a plexiglass screen (screen width: 61 cm) located inside the scanner at a distance of 73 cm from the participant. A cardboard with a midline horizontal aperture was placed in front of the VPixx projector to restrict its beam within a rectangular area [about 10 cm (height) x 60 cm (width), corresponding to 7.8° x 39.4° of visual angle] containing the stimuli, in order to reduce light intensity for the participant's comfort. Subjects could view the back-projected stimuli onto the plexiglass screen through the same head-coil mirror used for eye monitoring. All visual stimuli (except for EyeLink calibration: see above) were presented along an horizontal meridian centered within the 7.8° aperture, at an eccentricity varying between +/- 15° in Localizer blocks or between -8°/+17° in Experimental blocks.

2.3. General design

The top row of Figure 1 represents the timeline of the experiment. It comprised two 'localizer' functional runs (LOC) to identify regions of interest (ROIs) related to visuo-saccadic processing, an anatomical run (ANAT), and the five 'experimental' functional runs (EXP) to assess our main hypotheses. Each LOC run contained 181 MRI scans (5 min and 53 sec), each EXP run comprised 242 scans (7 min and 52 sec), the anatomical run contained 224 scans (11 min and 12 sec). Thus, a scanning session amounted to roughly 1h, including additional scans not shown in the figure (alignment and localisation scans, followed by field map images acquired for offline compensation of geometric distortions due to the inhomogeneity of the magnetic field B_0). All functional scans were T2*-weighted Echo Planar Images (EPI), with the following parameters: TR = 1950 ms, TE = 30 ms, flip angle = 90 °, resolution = 2.4 x 2.4 x 2.4 mm. Each scanned volume (13.44 cm) was acquired in 56 slices with a multiband sequence (no gap, interleaved, acceleration factor of 2, credits for providing the sequence to CMRR, Center for Magnetic Resonance Research, Minnesota, USA). During functional runs, 3 dummy scans were launched before triggering the saccade tasks. The experimenter could supervise in real-time the experiment by monitoring the MRI scans, the visual display, the eye movements recordings and the potential occurrence of head movements (FIRMM, NOUS Imaging). During the anatomical run, T1-weighted anatomical scans (TI = 1100 ms, TR = 3000 ms, TE = 3.7 ms, flip angle = 8°, resolution = 0.8 x 0.8 x 0.8 mm) were acquired. Between each run, participants were told about potential difficulties encountered in the preceding run (head motion, anticipations, blinks during crucial peri-saccadic periods) and were asked how they felt, if they wanted to rest and when they felt ready to proceed onto the next run.

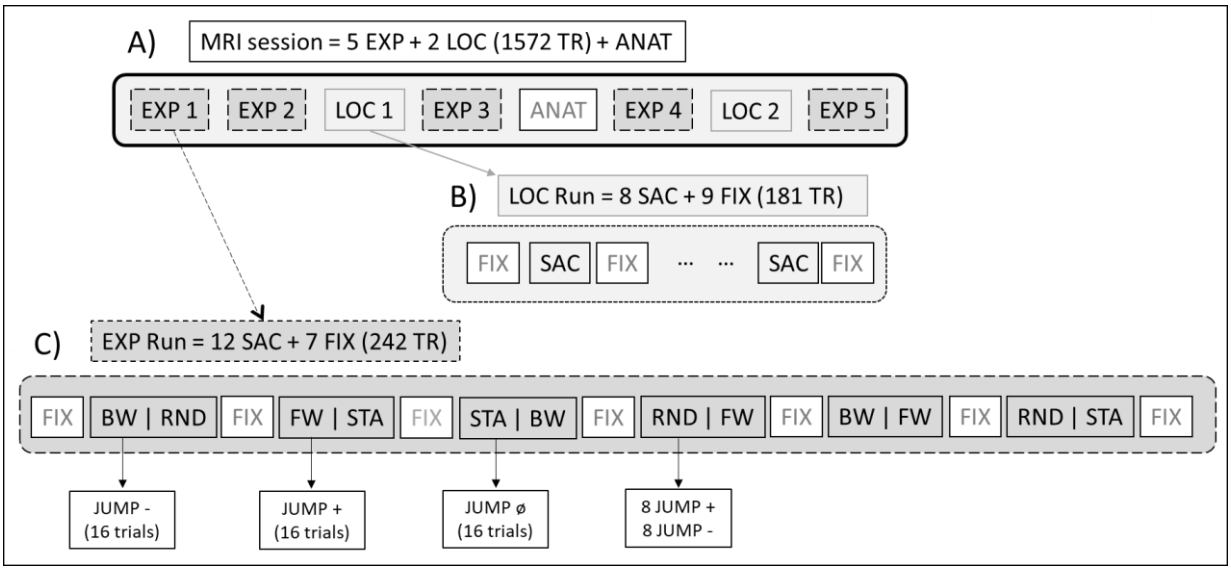

Figure 1. Experimental design. A)*: the sequence of the five experimental runs (EXP 1 to EXP 5: dark grey) interspersed with two localizer runs (LOC1 - LOC2: light grey) and an anatomical run (ANAT).* ***B)****: the localizer runs comprize 8 saccadic blocks and 9 fixation blocks.* ***C)****: the experimental runs contain three repetitions of the four conditions [BW: backward jump (-), FW: forward jump (+), RND: random jump (+/-), and STA: stationary, i.e. without target jump (ø)], yielding 12 saccade blocks of 16 trials each, interleaved with 7 fixation blocks. TR = number of MRI scans (TR duration = 1950 msec).*

2.3.1. Experimental runs

To assess our main hypotheses, four types of saccade blocks designed to induce different neurophysiological processes (see 2.4.1.Overview of fMRI analyses) were presented three times in each of the five experimental runs ('EXP 1' to 'EXP 5' in Figure 1). These saccade blocks corresponded to the following four conditions: FW-blocks containing 16 saccade trials with a forward target jump (FW-trial), BW-blocks containing 16 saccade trials with a backward target jump (BW-trial), RND-blocks containing a random sequence of eight FW-saccade trials and eight BW-saccade trials, and STA-blocks containing 16 trials of saccades without any target jump. The order of the saccadic block types (or saccade conditions) was randomized within each repetition and between runs and subjects. Each saccadic trial began in a similar manner: participants had to look at a visual point (dark circle of 1° of visual angle on the screen grey background) presented to the left and at an 8° eccentricity relative to the center of the screen (-8°). After a random fixation time (from 300 to 1500 ms), the fixation point was switched off and simultaneously a target appeared to the right at +8° or +12° of the screen center (16° or 20° from the fixation point, respectively) in a randomized order between trials and subjects (see Figure 2B top). Participants then had to execute a saccade in response to this first target displacement. As soon as this primary saccade was detected and while the eyes were still moving (online velocity threshold: 22°/sec and acceleration threshold = 4000 °/s/s), the target either jumped a second time to the left (backward, see Figure 2A top) or to the right (forward, see Figure 2A bottom) by 25% of the initial target eccentricity (i.e. 4° or 5° for a 16° or 20° initial jump, respectively;

see Figure 2B bottom), or remained stationary. Finally, after a random time (from 150 to 900 ms) the target disappeared and the participants were asked to move their gaze back to the original fixation point and to blink if needed. Note that the randomization of the duration of the fixation point and of the jumped target led to a total trial duration which on average equalled the MRI scan duration (TR= 1950 msec) but which varied between trials (from 1250 to 2900 ms), thus leading to a jitter between the scanning sequence and the saccadic task. Finally, each experimental run also comprised seven fixation (FIX) blocks (lasting six to eight MRI scans) in which subjects had to look at a stationary fixation point at the center of the screen. The order of the FIX-blocks was the following: one at the beginning, one at the end and the remaining five after every two saccade blocks.

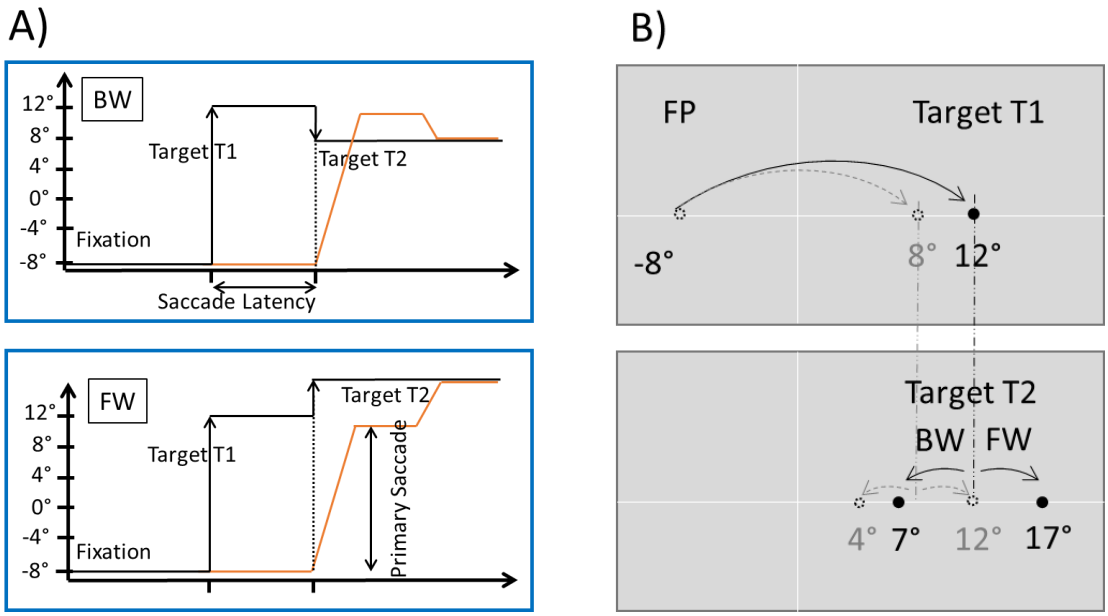

Figure 2. The target double-step paradigm. A) *temporal schematics of a backward trial (upper panel) and of a forward trial (lower panel). Fixation point and primary target (T1) presented respectively at -8° and 12° on the horizontal axis, secondary target (T2) presented during the saccade at 7° or 17° (jump of -5° or +5°).* ***B)*** *spatial schematics of the fixation point (FP) and targets (T1/T2) configurations in backward (BW) and forward (FW) trials: T1 at 12° jumps to T2 at 7° or 17°, or T1 at 8° jumps to T2 at 4° or 12° (in all cases corresponding to a 25% jump).*

2.3.2. Localizer runs

To identify regions of interest (ROIs) related to visuo-oculomotor control for the analysis of blood-oxygen-level dependent (BOLD) signals recorded in the 5 experimental runs (see '2.4.3. Overview of fMRI analyses'), participants also performed two localizer runs ('LOC1' and 'LOC2' in Figure 1). Each localizer run consisted in eight saccade blocks (16 scans each) intermingled with nine fixation blocks (five to eight scans, fixation point remaining at the center of the screen). In saccade blocks, a visual target was displayed in a fast pace [one presentation every 400 to 850 ms (mean = 650 msec) where the saccade target for a given trial acted as the fixation point for the next trial (Gray

et al., 2014)] at seven possible positions along the horizontal meridian (0°, +/-5°, +/- 10° or +/-15°). There were 48 target presentations per block, i.e. four pseudo-random sequences of 12 target presentations, each sequence containing six different target displacements (5° Left, 5° Right, 10° Left, 10° Right, 15° Left, 15° Right) repeated twice. There was no intra-saccadic target jump during saccades.

2.4. Data analysis

2.4.1. Eye-movement analysis

Oculomotor data of experimental runs (horizontal position of right eye, see examples in Inline Supplementary Figure 1) were analysed offline with a lab-made routine in Matlab R2015b (MathWorks Inc., Sherbom, MA). First, instantaneous eye velocity was obtained by temporal derivation of the position signal, then primary saccades were automatically detected based on a 45°/sec eye velocity threshold. After a systematic visual check, the starting and ending positions of each saccade, as well as the corresponding time values, were extracted. Trials were manually discarded when: a blink occurred during or just before the saccade, the saccade amplitude was less than half of the target distance, or the latency (time between the target appearance and the start of the saccade) was lower than 100 ms or greater than 500 ms. Trials with an EyeLink signal loss at a critical period were also discarded. In total, across subjects and conditions, 9.2 +/- 7.7% (mean +/- SD) of the trials were discarded, corresponding to 218 +/- 20 remaining valid trials (out of 240) in the FW condition, 217 +/- 17 in the BW condition, 220 +/- 17 in the RND condition and 217 +/- 21 in the STA condition.

For each trial, saccade horizontal amplitude was calculated as the difference between the horizontal starting and ending positions of the saccade, the gain as the ratio between horizontal saccade amplitude and desired saccade amplitude (distance between the saccade starting position and the first target position). The change of saccade gain was measured for each block of each run (n=12 x 5) by the slope of the linear regression between saccade gain and trial number (16 trials) within the block (see examples in Inline Supplementary Figure 2); saccade gain change was calculated separately in each participant and then averaged across participants. Statistical analyses were performed with Statistica (Statsoft, V13.5.0.17).

2.4.2. fMRI data pre-processing

All fMRI data were processed on SPM12 software (Wellcome Centre for Human Neuroimaging; https://www.fil.ion.ucl.ac.uk/spm/software/) in MATLAB environment. All DICOM scans were converted into NIfTI files, using the dcm2nii function of SPM12, except the 2 first ones of each functional run which were discarded to account for the scanner preparation time. A standard pre-

processing procedure was applied, including correction of head movements (the 6 estimated movement parameters - 3 translations along the reference planes and 3 rotations around the orthogonal reference axes - were later included as covariates in the design matrix of the general linear model (GLM) analyses), correction of geometric distortions (with a Voxel Displacement Map (VDM) created by estimating the inhomogeneity of the magnetic field B_0); then the images were resliced, co-registered, segmented, and normalised to MNI space. Spatial smoothing (Gaussian kernel of 6 mm full width at half maximum) was only applied for the whole brain GLM analyses, including those used for ROIs definition, but for MVPA non-smoothed images were used instead (see Haynes and Rees 2006; Gerardin et al 2012).

2.4.3. Overview of fMRI analyses

The data collected in the 5 experimental runs were submitted to a whole-brain GLM analysis and to a set of ROI-based MVPAs. ROIs were functionally identified based on another whole brain GLM of independent data collected in the 2 localizer runs. Then, for each ROI and participant, the 100 most active voxels were selected; finally, the activation levels of these 100 voxels determined in three event-related whole-brain GLM analyses of non-smoothed experimental data were used to feed the MVPAs (see details below). The rationale of fMRI analyses (GLM contrasts or MVPA classifications) was the following. The four conditions (FW, BW, RND, STA) were intended to elicit specific neurophysiological processes : STA = planning and execution of leftward saccades; RND = planning and execution of leftward saccades + processing of target error in both directions (elicited by intra-saccadic target step randomly to the left or to the right); FW (or BW) = planning and execution of leftward saccades + processing of consistent target error and adaptation in the forward (or backward) direction [elicited by intra-saccadic target step systematically to the right (or left)]. Note that some additional neurophysiological processes can be more directly related to the intra-saccadic target perturbation itself (FW, BW and RND), to endogenous errors unrelated to intra-saccadic target jump (STA) and to some very fast component of adaptation in RND (effect of target jump in trial n on saccade in trial n+1 : see Srimal et al., 2008). However, although we cannot fully rule them out, these additional effects will negligibly impact our fMRI results and will be overcome by the large differences of neural processing delineated in the following planned comparisons, whether based on GLM contrasts or MVPA classification procedures. First, comparisons of the combined FW and BW trials versus STA trials (FW + BW vs STA) should disclose neural substrates of adaptation and/or error processing unrelated to direction, and comparisons between combined FW and BW trials versus RND trials (FW + BW vs RND) should disclose substrates of adaptation only, again unrelated to direction. Second, the delineation of error processing substrates should be revealed by comparing RND to STA (RND vs STA). Third, to gain insight into the mechanisms specifically related to

the direction of adaptation, comparisons of FW (or BW) trials versus STA trials should reveal substrates of adaptation and/or error processing in the forward (or backward) direction, whereas comparisons of FW trials versus RND+ trials (or BW trials versus RND- trials) should reveal substrates of adaptation only and in the forward (or backward) direction. A summary of all GLM analyses and MVPAs is provided in the Inline Supplementary Table 1.

2.4.4. GLM-1: block-design whole-brain GLM analysis of experimental runs

We first performed a block-design whole-brain GLM analysis (hereafter called GLM-1) of the experimental runs for each subject (first level analysis) and used the results for a second GLM at the group level (second level analysis). The design matrix was the same for all subjects except for subject 12 where one run was discarded from both fMRI and eye movement analyses due to a critical loss of eye signals. This design comprised, for each run, the five conditions (FW/BW/RND/STA/FIX) which were used as interest regressors and the six head movement parameters which were included as non-interest regressors. The onsets of the conditions were defined as the start time of the first trial of each block (fixation point presentation), and the duration was set to the duration of the block (16 scans for saccadic blocks, 5-8 scans for fixation blocks). All condition blocks were modelled as box-car functions and convolved with the Hemodynamic-Response-Function (HRF).

The rationale to disclose at the whole-brain level the neural areas related to saccadic adaptation and error signals processing is as follows: FW blocks involve adaptation and error signals in the forward direction, BW blocks involve adaptation and error signals in the backward direction, RND blocks involve bi-directional error signals, and STA blocks involve saccade behaviour with no adaptation and no error signal. Hence, activations related to adaptation ('Adaptation') and error signals processing ('Error') were estimated at the subject level by the following five t-contrasts: 1) the (FW & BW) > STA contrast estimated the global activation related to adaptation and/or error signals ('Adaptation + Error'); 2) the (FW & BW) > RND contrast estimated the activation related specifically to adaptation ('Adaptation'); 3) the RND > STA contrast estimated the activation related specifically to error signals ('Error'); 4) the FW > STA contrast estimated the activation related to saccadic adaptation and/or error in the lengthening (FW) direction ('Adaptation + Error FW'); 5) finally the BW > STA contrast identified activation related to saccadic adaptation and/or error in the shortening (BW) direction ('Adaptation + Error BW'). For each contrast, the results of these 24 individual-level analyses were entered in a group-level analysis (paired t-test).

2.4.5. GLM-2: block-design whole-brain GLM analysis of experimental runs

The same block-design whole-brain GLM analysis (hereafter called GLM-2) of the experimental runs was again performed for each subject (first level analysis), but this time on non-spatially

smoothed data, to provide data set (beta values) for the ROIs-based multivoxel pattern analyses (MVPAs). Also, instead of the t-contrasts between the different conditions computed by GLM-1 (e.g. FW & BW > STA), in GLM-2 the t-contrasts of each condition relative to fixation were extracted (e.g. FW & BW > FIX and STA > FIX) to produce the beta values required by MVPA pair-wise comparisons (e.g. FW & BW vs. STA).

2.4.6. Block-design whole-brain GLM analysis of localizer runs

Another block design whole-brain GLM analysis was conducted on the localizer runs to identify the regions of interest (ROIs) for the multivoxel pattern analysis (MVPA). The processing steps were the same as described above for the analysis of the experimental runs (GLM-1) except that the two conditions of the localizer runs (SAC/FIX) were used as interest regressors (non-interest regressors involved again the six movement parameters). The SAC vs. FIX t-contrasts were calculated at the group-level (p-threshold of 0.001, no voxel extent threshold) to identify cortical and sub-cortical areas involved in processing visual and/or oculomotor signals for saccade planning and execution. These clusters were later used to identify the ROIs on which MVPAs were performed (see Results section).

2.4.7. Event-related whole-brain GLM analyses of experimental runs

The following three event-related whole-brain GLM analyses of non-smoothed data were performed to feed the MVPAs detailed in the paragraph below (2.4.8. MVPA analyses).The first one (hereafter called GLM-3.1) was designed to investigate the direction of the error signal, differentiating in the RND blocks the trials with a forward target jump (RND+) from those with a backward jump (RND-). This event-related analysis was defined with one event per behavioural trial, with the onset synchronized to the presentation of the first target and the duration set to 0, each trial being modelled as a delta function and convolved with the HRF. In addition to RND+ and RND- trials, the 4 other types of trials (conditions FW, BW, STA, FIX) were also included and defined with the same event-design, allowing us to provide the t-contrasts needed to perform the following pair-wise MVPA comparisons: RND+ vs. STA; RND- vs. STA; FW vs. RND+; and BW vs. RND-. As in the previous GLMs, the six movement parameters were included as non-interest regressors.

A second event-related GLM (hereafter called GLM-3.2) was created as a test complementing GLM-2 and GLM-3.1. GLM-3.2 aimed at identifying neural areas involved in the processing of absolute post-saccadic target error (between saccade endpoint and final target position). This parameter was estimated across the different conditions, thus quantifying the size of error signals due to the combined effects of target jumps and of natural fluctuations of saccade amplitude. The distribution of this parameter was obtained for each subject and each run. Based on these

distributions, two groups were defined which contained respectively 25% of trials (48 trials per run and per subject) with the largest saccade error ('High error' group, grand mean =5.4° +/- 0.25°) and 25% of trials with the smallest error ('Low error' group, grand mean =0.8° +/- 0.21°). 'High error' trials, 'Low error' trials and Fixation trials (event duration = 0, event onset = presentation of the first target or fixation trial onset) were modelled again as delta function convolved with the HRF and included as three regressors of interest, all remaining trials and all movement parameters being set as regressors of non-interest.

Finally, a third event-related GLM (hereafter called GLM-3.3) was designed in order to check whether areas deemed to be involved in adaptation processes are not in fact merely encoding saccade metrics (absolute saccade size). Similar to GLM-3.2, GLM-3.3 differentiated two groups of trials based on the distributions of saccade gain calculated for each subject and each run, containing respectively 25% of trials with the largest saccade gain ('High amplitude' group, grand mean gain = 0.84° +/-0.07°, mean amplitude estimated for a theoretical saccade toward a 18° target = 15.1°) and 25% of trials with the smallest saccade gain ('Low amplitude' group, grand mean gain = 0.72° +/- 0.06°, mean amplitude for a theoretical 18° saccade = 13.0°).

2.4.8. fMRI: MVPA analyses

We first selected 34 spherical regions of interest (ROIs) based on clusters identified by the whole-brain GLM analysis of the localizer runs (see results in section 3.3). Then, for each ROI and each participant, the 100 most active voxels in that GLM localizer contrast were identified. Finally, again for each ROI and each participant, we created datasets filled with the beta-values of these 100 voxels resulting from each of the four whole brain GLM analyses performed on non-smoothed data (GLM-2, GLM-3.1, GLM-3.2, GLM-3.3). These four whole brain GLM analyses were used as inputs for different MVPA classifications (see Inline Supplementary Table 1): (A) the block-design GLM-2 analysis with the FW, BW, RND, STA and FIX blocks provided a dataset with five predictors per run (obtained respectively from the following five contrasts: FW> FIX, BW > FIX, RND > FIX, STA > FIX and FW & BW > FIX); (B) the event-related GLM-3.1 analysis with the FW, BW, RND+, RND-, STA and FIX trials as events led to a dataset of five predictors per run (obtained respectively from the following five contrasts: FW> FIX, BW> FIX, RND+ > FIX, RND- > FIX, and STA>FIX); (C) the event-related GLM-3.2 analysis with High error, Low error, and FIX trials as events gave a dataset composed of two predictors per run (obtained respectively from the High error > FIX and Low error > FIX contrasts); (D) the event-related GLM-3.3 analysis with High amplitude, Low amplitude and FIX trials as events gave a dataset composed of two predictors per run (obtained respectively from the High amplitude > FIX and Low amplitude > FIX contrasts).

The beta values of each voxel were z-score normalised run by run, then only the data corresponding to the two conditions of interest of each pair-wise MVPA classification were kept.

We used a Support Vector Machine (SVM) classifier and we performed for each search between the two conditions of interest a "leave-one-run-out" cross-validation procedure: the classifier was trained on four runs and tested on the remaining one. This procedure was repeated for all the runs, i.e. five classification rounds were performed, the final classification accuracy being the mean performance over these five rounds (chance level= 0.5).

The results were corrected for multiple comparisons with Monte-Carlo based clustering statistics, following a CoSMoMVPA built-in function (Oosterhof et al., 2016). As shown in Inline Supplementary Figure 3, a total of 10,000 comparisons were performed with Threshold Free Cluster Enhancement (TFCE) between the original set of classification accuracies and a null distribution of classification accuracies randomly drawn from 100 null-datasets. Each null-dataset was computed by randomizing the conditions' labels and launching the SVM classifier with these newly-labelled conditions. The 10,000 TFCE calculations resulted in a final z-score for each ROI and each pair-wise classification: the ROI's classification accuracy was judged to be significantly larger than 0.5 after correction for multiple comparisons whenever the z-score was above 1.65 (alpha=0.05). We also calculated from the z-score the equivalent p-value.

As described in the Results section (see also Inline Supplementary Table 1), we performed two independent analyses of these results: one focused on the delineation between adaptation vs. error signal (MVPA-1), and the other aiming to differentiate between forward vs. backward directions (MVPA-2). For this, we considered six pair-wise classifications in MVPA-1 and six pair-wise classifications in MVPA-2, so in both cases we applied a further correction for multiple comparisons (Bonferroni, n=6).

3. RESULTS

This study had two main objectives: first, to determine the neural substrates of saccadic adaptation per se and of error signal processing and second, to determine whether these cortical and sub-cortical substrates differ according to the direction (forward versus backward) of adaptation. In the following, we first report behavioural measures to check whether adaptation of reactive saccades was readily induced during the FW and BW blocks of trials (systematic intra-saccadic target jumps) compared to the RND block (random target jumps eliciting saccade errors) and the STA block (no jump: control saccades toward stationary target). We then present the neuroimaging data collected

during these Experimental runs, using analyses of BOLD signal relying both on whole brain GLM approaches and on ROIs-based MVPAs (ROIs defined based on BOLD signal from Localizer runs).

3.1. Behavioral measures: Saccadic adaptation

We determined the effect of adaptation by computing the gain change within each block as the slope of the gain vs. trial number linear fit (see Inline Supplementary Figure 2 for a representative example in each condition). We submitted the saccadic gain change to a repeated measures ANOVA (rmANOVA) with the three within-subject factors: run (EXP1, EXP2, EXP3, EXP4, EXP5), condition (FW, BW, RND, STA) and repetition of the condition within an experimental block (repetition 1, repetition 2, repetition 3). This rmANOVA revealed a main effect of condition ($F(3,60)=226.41$; $p<10E-6$, $\eta^2=0.92$) and a significant interaction between condition and repetition ($F(6,120)=2.90$; $p=0.011$, $\eta^2=0.13$), in addition with a significant triple interaction run x condition x repetition ($F(24,480)=1.89$; $p=0.007$, $\eta^2=0.09$). All other main effects or interactions were not significant (all $F< 1.5$ and $p> 0.13$). Note that the main effect of condition was way stronger than the double and triple interaction effects (see corresponding η^2 values). This pattern of results is consistent with the adaptation being consistently induced in the BW and FW conditions and yielding much stronger gain changes than in the RND and STA conditions. Indeed, as shown in Figure 3, post-hoc comparisons revealed that the slope in both BW and FW conditions (means of $-3.35x10^{-3}$ and $2.79x10^{-3}$ corresponding to mean gain changes between trials 1 and 16 of -0.054 and 0.045, respectively) was significantly steeper than in the RND and STA conditions (Bonferroni tests, all $p < 10E-6$). The triple interaction effect seems to be due to the largest gain decrease during the first repetition of the BW condition in EXP1 and EXP3, and the largest gain increase during the third repetition of the FW condition in EXP4, a pattern also consistent with the double interaction.

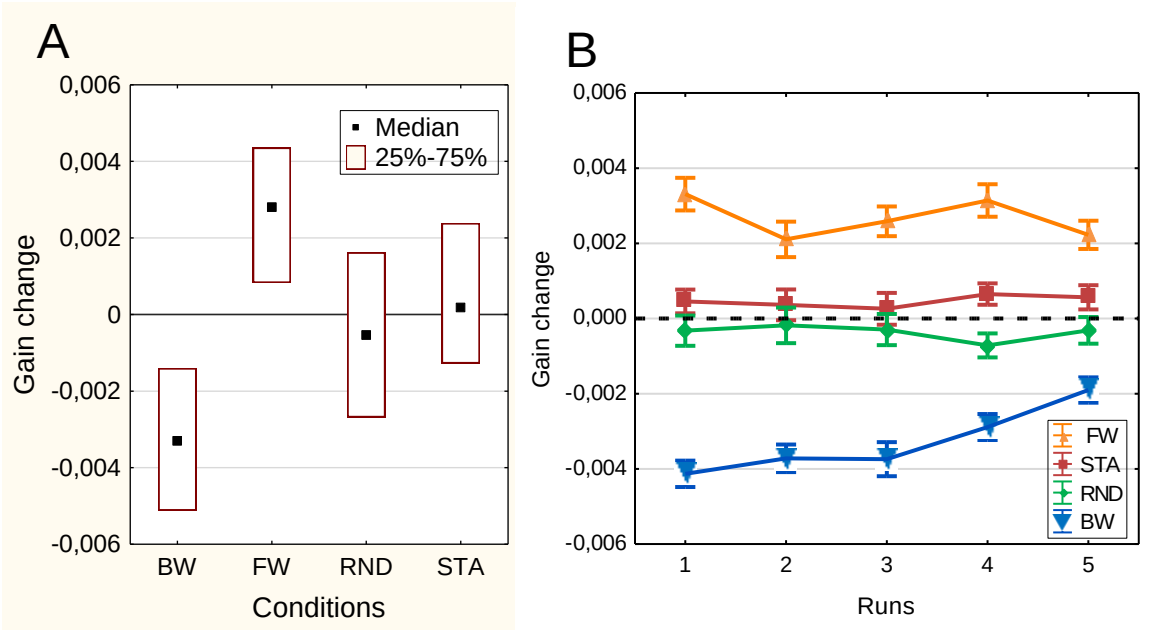

Figure 3. *Saccade gain change in the 4 conditions.* ***(A)*** *Overall gain change across runs plotted for the 4 conditions (median and 25-75 percentil range).* ***(B)*** *Mean gain change for the 4 conditions plotted for the 5 experimental runs (error bars = standard errors of the mean).*

The results of the same ANOVA submitted separately to the saccadic gain and the saccadic latency are reported in the Inline Supplementary data.

3.2. fMRI: Whole-brain univariate analysis of Experimental runs

For each of the five contrasts of the GLM-1 analysis (see Material and Methods section: 'Adaptation', 'Adaptation + Error', 'Adaptation + Error BW', 'Adaptation + Error FW', 'Error'), statistical maps were computed with a voxel-level p-value of p<0.001 and a cluster-level p-value corrected for multiple comparisons (Family Wise Error correction) p_{FWE_corr} <0.05 (see Table 1). In the 'Adaptation' contrast (FW & BW > RND), only a significant cluster was found in the left temporal area. No significant activation was found in the 'Adaptation + Error' contrast (FW & BW > STA). In the direction-specific 'Adaptation + Error BW' and 'Adaptation + Error FW' contrasts, the right occipital cortex was activated for the backward direction (BW > STA), whereas a large and bilateral cluster was found in the occipital cortex for the forward direction (FW > STA). Finally, for the 'Error' contrast (RND > STA), two significant clusters were found in the left hemisphere, one in SPL and the other corresponding to the PEF (see Inline Supplementary Figure 5).

		MNI coordinates				
Contrasts	**Anatomical Location**	**X**	**Y**	**Z**	**cluster size**	**p_{FWE_corr}**
Adaptation	L-Inf_Temp	-42	-9	-24	137	0.004
Adaptation + Error BW	R-Occ	18	-93	-3	301	<0.001
Adaptation + Error FW	L-Occ	-1	-88	7	●	●
Adaptation + Error FW	R-Occ	11	-62	-3	●	●
Error	L-PEF	-37	-45	48	147	0.003
Error	L-SPL	-16	-64	64	84	0.041

● Large cluster (1003 voxels, p<0.001) with reported L-OCC and R-OCC peaks

Table 1. *Whole-brain univariate results of experimental runs (group analysis, N=24). MNI coordinates, cluster size and FWE-corrected p-values of clusters showing significant activation for the following contrasts: FW & BW > RND (Adaptation), BW > STA (Adaptation + Error BW), FW > STA (Adaptation + Error FW), RND > STA (Error). No significant cluster was found for the FW & BW > STA contrast (Adaptation + Error). L-inf_Temp: Left inferior temporal cortex; R-Occ and L-Occ: right and left occipital cortex; L-PEF: left parietal eye field; L-SPL: left superior parietal lobule.*

3.3. fMRI: Whole-brain univariate analysis of Localizer runs: ROIs definition

Regions of interest (ROIs) were identified as cortical and sub-cortical areas which were significantly more active during the saccade blocks than during the fixation blocks of the localizer

runs, or *vice versa*. To this aim, a whole-brain GLM analysis was performed and saccade vs. fixation contrasts were computed at the group-level (p-threshold of 0.001 and no voxel extent threshold). A total of 30 clusters was identified (see Figure 4 and Inline Supplementary Table 2): 12 pairs of clusters identified in both hemispheres, 2 medial clusters, and 4 clusters identified in only the right hemisphere (DLPFC, thalamus, pallidum) or the left hemisphere (frontal gyrus). Most of these 30 clusters reached significance level with $p_{FWE\_corr}<0.05$, except three which were slightly below but which we considered of interest for the present study based on the literature (van Broekhoven et al., 2009; Liem et al 2012; Srivastava et al 2019): right angular gyrus ($p_{FWE\_corr}=0.058$), left inferior cerebellum ($p_{FWE\_corr}=0.051$) and right inferior cerebellum ($p_{FWE\_corr}=0.102$). Also, we delineated 4 additional clusters as the contralateral counterparts of the 4 clusters found in only one hemisphere by flipping their X coordinate, yielding a total of 34 clusters. To conduct the MVPA analysis described in the following paragraph, a spherical ROI was created for each of these 34 clusters and centered on the maximally-activated voxel in the cluster (MarsBaR toolbox, Brett et al., 2002). A radius of 10 mm was applied for cortical ROIs and of 8 mm for subcortical ROIs (cerebellum, thalamus, pallidum). This yielded in every subject at least 100 voxels activated in the saccade vs. fixation contrasts of the localizer (no voxel extent threshold, uncorrected p-threshold of 1), except for the left pallidum: hence the radius of both left and right pallidum ROIs was increased to 10 mm. Finally, for each subject and each ROI, the 100 most active voxels were selected.

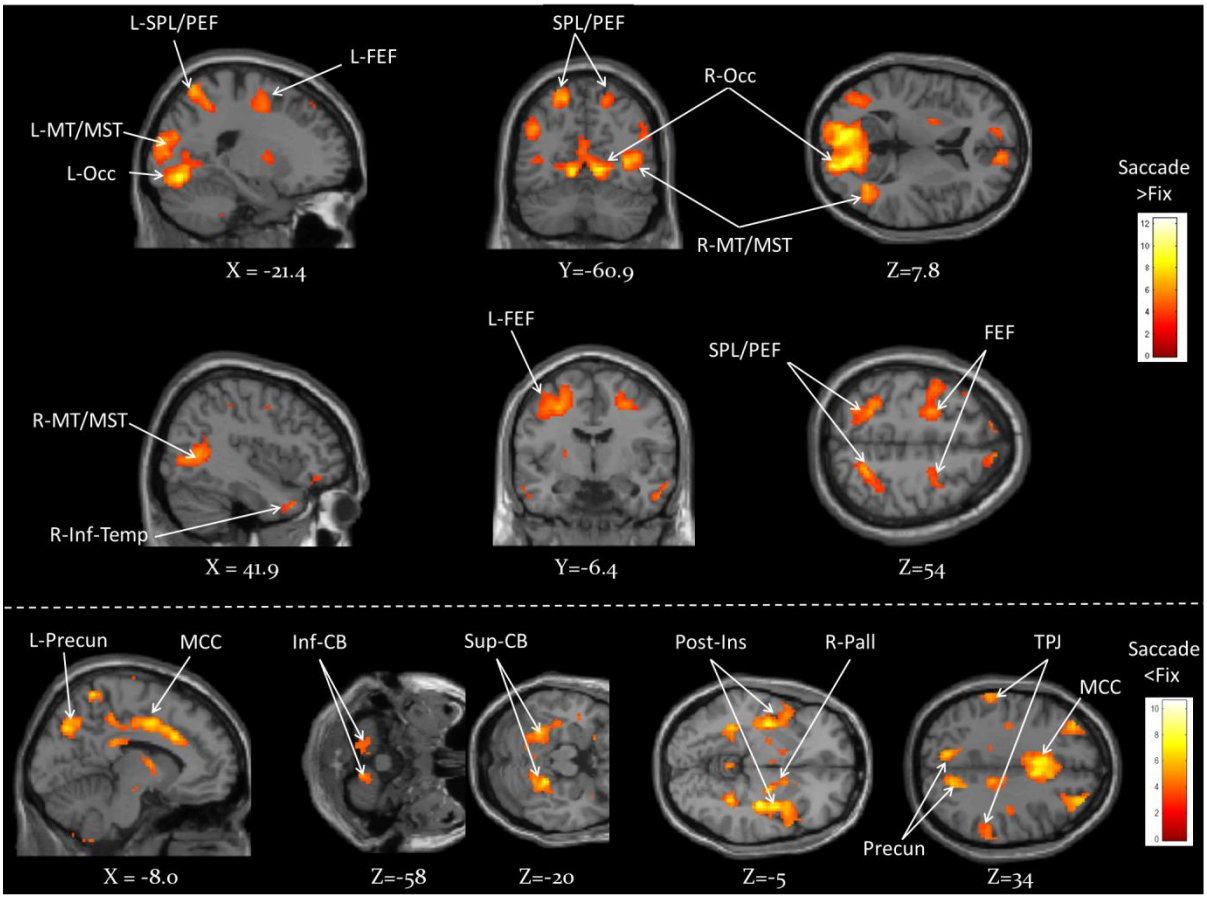

Figure 4. Visuo-saccadic network identified by whole-brain GLM of Localizer runs*. Results of Saccade > Fixation contrast (upper two rows) and of reverse contrast (Fixation > Saccade, 3d row). Twelve pairs of clusters were identified across hemispheres (one not shown: angular gyrus), 4 clusters only in the right hemisphere (pallidum, and 2 not shown: DLPFC, thalamus) or the left hemisphere (frontal gyrus), and 2 medial clusters (one not shown: orbitofrontal cortex). See text for details.*
Abbreviations: Occ: occipital; MT/MST: medial temporal & medial superior temporal; inf_Temp: inferior temporal; PEF: parietal eye field; SPL: superior parietal lobule; FEF: frontal eye field; TPJ: temporo-parietal junction; Precun: precuneus; MCC: middle cingulate cortex; Post-Ins: posterior insula; Pall: pallidum; Inf-CB: inferior cerebellum; Sup-CB: superior cerebellum.

3.4. ROIs-based MVPA-1: adaptation vs. error signals processing

As stated in the Material and Methods section, we performed two independent analyses focusing respectively on the delineation between adaptation vs. error signal (MVPA-1) and between forward vs. backward directions (MVPA-2). We used a multiple criteria approach involving six pair-wise classifications in MVPA-1 and six pair-wise classifications in MVPA-2, applying in both cases a Bonferroni correction for multiple comparisons (n=6, p-value < 0.0083).

For the identification of ROIs related to saccadic adaptation (Table 2), at least one of these three criteria was necessary: significant discrimination (1) between FW & BW vs. RND conditions (identifying areas related to adaptation in general), (2) between FW vs. RND+ conditions (areas related to forward adaptation), or (3) between BW vs. RND- conditions (areas related to backward

adaptation). As can be seen in Table 2, five out of the 34 tested ROIs met at least one criterion (i.e. a Bonferroni-corrected p-value of classification performance <0.05). Both left and right temporo-occipital cortices (L-MT/MST and R-MT/MST), as well as the right FEF, significantly discriminated between FW & BW and RND. Examination of the two other, direction-specific, criteria, further disclosed that the right temporo-occipital cortex (R-MT/MST) was involved in backward adaptation whereas the homologous area (L-MT/MST) was involved in forward adaptation. Finally, two other ROIs were disclosed for a single adaptation direction: the right pallidum (R-Pall) in forward adaptation and the right occipital cortex (R-Occ) in backward adaptation.

		GLM-2: FW & BW vs. RND (Adaptation)	GLM-3.1: FW vs. RND+ (Adaptation FW)	GLM-3.1: BW vs. RND- (Adaptation BW)
R-Occ	Accuracy	0.54 +/- 0.11	0.55 +/- 0.12	**0.59 +/- 0.08**
	p-value	0.5	0.5	**0.0006**
R-MT/MST	Accuracy	**0.61 +/- 0.11**	0.55 +/- 0.09	**0.58 +/- 0.08**
	p-value	**0.0025**	0.1460	**0.003**
L-MT/MST	Accuracy	**0.61 +/- 0.12**	**0.58 +/- 0.08**	0.59 +/- 0.11
	p-value	**0.0037**	**0.0021**	0.0085
R-FEF	Accuracy	**0.59 +/- 0.11**	0.52 +/- 0.10	0.53 +/- 0.09
	p-value	**0.0053**	0.5	0.5
R-Pall	Accuracy	0.54 +/- 0.07	**0.56 +/- 0.07**	0.54 +/- 0.06
	p-value	0.1492	**0.0016**	0.1617

Table 2. ROIs related to saccadic adaptation*. These 5 ROIs significantly discriminated FW & BW vs. RND, FW vs. RND+, or BW vs. RND-. Accuracy: mean discrimination accuracy (+/-SD) across the 24 subjects; p-value: Bonferroni-corrected p-values converted from the Z-scores of the Monte-Carlo based clustering approach. Significant results (p-value < 0.0083) are highlighted in bold. Abbreviations: Occ: occipital; MT/MST: medial temporal & medial superior temporal; FEF: frontal eye field; Pall: pallidum.*

There is a possibility that some of these ROIs deemed to be involved in saccadic adaptation processes might in fact host neural processes that take place during adaptation but are not directly related to saccadic adaptation. For example, even though unrelated to saccadic plasticity mechanisms, ROIs that encode saccade amplitude are expected to be recruited during saccadic adaptation phases. To address this possibility, we performed an additional MVPA using the output of GLM-3.3 (see Materials and Methods) to test whether any of the 34 ROIs could discriminate between 'High amplitude' vs. 'Low amplitude' saccades. The results disclosed no significant discrimination for any of the ROIs, including those reported in Table 2. Note that this negative result is unlikely due to insufficient sensitivity as the mean difference of gain between these two populations of saccades (0.12) was larger than the mean change of gain during BW and FW blocks (see above: 0.099) which nonetheless led to significant MVPA results. In conclusion, this analysis suggests that ROIs listed in

Table 2 are likely related to saccadic adaptation processes and not to the resulting change of saccade size.

For the identification of ROIs involved in error signals processing (Table 3), we used as first and necessary criterion a significant discrimination between FW & BW vs. STA conditions without significant discrimination between FW & BW vs. RND conditions; the other two criteria were a significant discrimination between RND vs. STA or between High error vs. Low error, respectively. The first criterion was met by six out of 34 ROIs (L-Occ, L-PEF, L-Precun, L-Inf-CB, R-Sup-CB and MCC), among which two (L-Occ, L-PEF) additionally fulfilled the "High error vs. Low error" discrimination criterion (see Table 3 for details). No ROI additionally fulfilled the 2nd criteria (RND vs. STA).

		GLM-2: FW & BW vs. STA (Adaptation+Error)	GLM-2: FW & BW vs. RND (Adaptation)	GLM-2: RND vs. STA (Error)	GLM-3.2: High_Error vs. Low_Error
L-Occ	Accuracy	**0.66 +/- 0.13**	0.56 +/- 0.09	0.64 +/- 0.18	**0.78 +/- 0.21**
	p-value	**0.0002**	0.0619	0.0157	**0.0001**
L-Precun	Accuracy	**0.60 +/- 0.11**	0.55 +/- 0.09	0.58 +/- 0.20	0.69 +/- 0.24
	p-value	**0.0059**	0.1492	0.5	0.0191
L-PEF	Accuracy	**0.64+/- 0.13**	0.58 +/- 0.13	0.55 +/- 0.23	**0.76 +/- 0.22**
	p-value	**0.0009**	0.1492	0.5	**0.0005**
MCC	Accuracy	**0.61 +/- 0.12**	0.55 +/- 0.09	0.55 +/- 0.22	0.53 +/- 0.30
	p-value	**0.0059**	0.1916	0.5	0.5
L-Inf-CB	Accuracy	**0.59 +/- 0.10**	0.54 +/- 0.13	0.54 +/- 0.17	0.46 +/- 0.30
	p-value	**0.0059**	0.5	0.5	0.5
R-Sup-CB	Accuracy	**0.59 +/- 0.09**	0.55 +/- 0.09	0.55 +/- 0.15	0.46 +/- 0.32
	p-value	**0.0017**	0.1916	0.5	0.5

Table 3. ROIs related to error signals processing*. Significant results (p-value < 0.0083) are highlighted in bold (same conventions as in Table 2). These six ROIs significantly discriminated FW & BW from STA but not FW & BW from RND (all p>0.0083), with two ROIs also discriminating between High error vs. Low error. The RND vs. STA discrimination did not reach significance for any ROI. Abbreviations: Occ: occipital; Precun: precuneus; PEF: parietal eye field; MCC: middle cingulate;Inf-CB: inferior cerebellum; Sup-CB: superior cerebellum.*

3.5. ROIs-based MVPA-2: forward vs. backward directions

To disclose which of the 11 just-described ROIs involved in adaptation and/or error signal are specifically related to the forward or backward direction, we used a multiple criteria approach based on six pair-wise MVPA discriminations, three encoding the forward direction (Table 4: 'Adaptation + Error FW', 'Error FW' and 'Adaptation FW) and three encoding the backward direction (Table 5: 'Adaptation + Error BW', 'Error BW' and 'Adaptation BW).

For the forward direction (Table 4), we relied on the "FW vs. STA", "RND+ vs. STA", and "FW vs. RND+" discriminations. The left occipital cortex (L-Occ) significantly discriminated between FW vs.

STA and between RND+ vs. STA conditions, whereas both L-MT/MST and right pallidum (R-Pall) significantly discriminated between FW vs. RND+ conditions.

		GLM-2: FW vs. STA (Adaptation + Error FW)	GLM-3.1: RND+ vs. STA (Error FW)	GLM-3.1: FW vs. RND+ (Adaptation FW)
L-Occ	Accuracy	**0.76 +/- 0.21**	**0.65 +/- 0.16**	0.55 +/- 0.10
	p-value	**0.0001**	**0.0022**	0.2404
L-MT/MST	Accuracy	0.59 +/- 0.18	0.58 +/- 0.13	**0.58 +/- 0.08**
	p-value	0.3797	0.1825	**0.0021**
R-Pall	Accuracy	0.46 +/- 0.19	0.54 +/- 0.08	**0.56 +/- 0.07**
	p-value	0.5	0.1825	**0.0016**

Table 4. ROIs related to the forward direction*. Significant results (p-value < 0.0083) are highlighted in bold (same conventions as in Tables 2 and 3).These three ROIs significantly discriminated FW vs. STA, or RND+ vs. STA or FW vs. RND+. Abbreviations: Occ: occipital; MT/MST: medial temporal & medial superior temporal; Pall: pallidum.*

For the backward direction (Table 5), the criteria used were the discriminations of the exact symmetrical conditions: "BW vs. STA", "RND- vs. STA" and "BW vs. RND-". Results displayed in Table 5 disclosed only two ROIs, R-Occ and R-MT/MST, which both met the criterion of a significant discrimination between BW vs. RND- conditions.

		GLM-2: BW vs. STA (Adaptation + Error BW)	GLM-3.1: RND- vs. STA (Error BW)	GLM-3.1: BW vs. RND- (Adaptation BW)
R-Occ	accuracy	0.56 +/- 0.23	0.53 +/- 0.10	**0.59 +/- 0.08**
	p-value	0.5	0.5	**0.0006**
R-MT/MST	accuracy	0.57 +/- 0.20	0.55 +/- 0.12	**0.58 +/- 0.08**
	p-value	0.5	0.5	**0.003**

Table 5. ROIs related to the backward direction*. Significant results (p-value < 0.0083) are highlighted in bold (same conventions as in Tables 2, 3 and 4). These two ROIs significantly discriminated BW vs. STA, or RND- vs. STA or BW vs. RND-. Abbreviations: Occ: occipital; MT/MST: medial temporal & medial superior temporal.*

4. DISCUSSION

4.1. Summary of results

The aim of the present study was to investigate the cortical and subcortical areas involved in both forward and backward adaptation of rightward reactive saccades, and to disentangle them from those specifically involved in encoding the visual error signals leading to adaptation. Our behavioral results indicate that exposure to the short blocks of systematic double-step targets successfully induced saccadic adaptation, in both the forward and backward directions. Our localizer task involving bi-lateral reactive saccades allowed us to reconstruct a wide visuo-saccadic network of cortical and subcortical structures (Figure 4 and Inline Supplementary Table 2), closely corresponding to the network identified over the years by complementary methods in both human (e.g. Grosbras et al., 2005; Lynch & Tian, 2006; Curtis & Connolly, 2008; McDowell et al., 2008; Domagalik et al., 2012; Bender et al., 2013; Herveg et al., 2014; Petit et al., 2015; Coiner et al., 2019) and non-human primates (see Munoz & Everling, 2004 for review). Then, as summarized in Figure 5, our main experimental task of rightward reactive saccades disclosed the involvement of various brain regions in adaptation mechanisms (bilateral MT/MST; the inferior temporal cortex in the left hemisphere; and in the right hemisphere: the occipital cortex, FEF and pallidum) and in error processing (in the left hemisphere: occipital cortex, PEF, SPL, precuneus, inferior cerebellum; in the right hemisphere: superior cerebellum; in the midline: cingulate cortex). Finally, a selectivity for the direction of adaptation could be established for the occipital cortex and MT/MST complex (left and right hemispheres for forward and backward, respectively) and the pallidum (right hemisphere for forward).

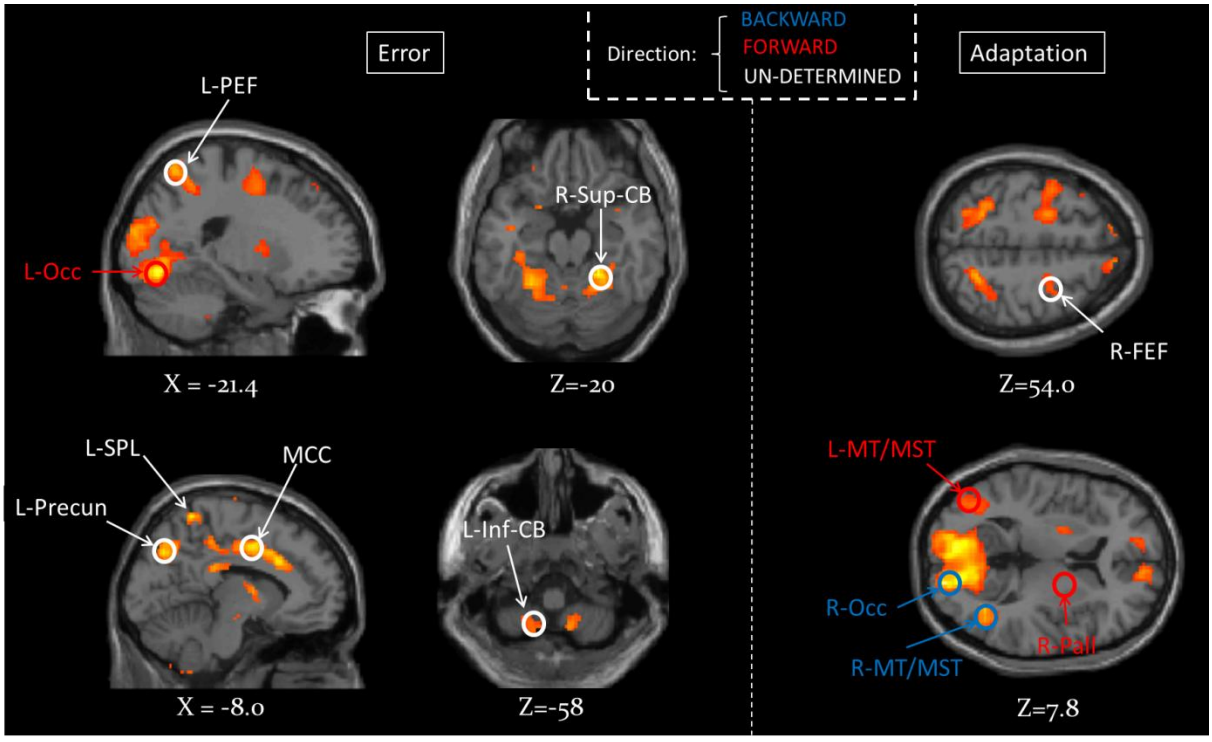

Figure 5. Summary of error-processing and adaptation networks*. Superimposed on the GLM maps of visuo-saccadic areas identified by Localizer runs (see Figure 4), circles show MVPA-determined ROIs significantly related to error processing (left) or to adaptation (right). Blue and red circles / labels denote selectivity to the BW and FW directions, respectively. The involvment of L-PEF, as well as the selectivity of L-Occ and R-Occ to FW and BW directions, respectively, were confirmed by GLM analyses (Table 1) which, in addition, also revealed 2 further clusters, one in L-SPL related to error processing (lower left) and in L-Inf-temp cortex related to adaptation (not shown). Abbreviations: Occ: occipital; MT/MST: medial temporal & medial superior temporal; PEF: parietal eye field; SPL: superior parietal lobule; FEF: frontal eye field; Precun: precuneus; MCC: middle cingulate cortex; Pall: pallidum; Inf-CB: inferior cerebellum; Sup-CB: superior cerebellum.*

4.2. Behavioral results

The saccadic gain significantly decreased during BW blocks and increased during FW blocks, consistent with backward and forward adaptation, respectively. Indeed the linear fits of gain change within BW and FW blocks disclosed negative and positive slopes, respectively, which both significantly differed from those computed in the RND and STA blocks. Note that the global saccadic gain in all 4 types of blocks decreased along the experiment. As detailed in Inline Supplementary data, the irregular pattern of such gain decrease across runs argues against a pure fatigue effect and rather suggests some temporal carry-over of the stronger saccade shortening achieved in BW blocks compared to the saccade lengthening in FW blocks. Finally, the values of the gain change slope in the FW and BW conditions (2.79x10-3 and -3.35x10-3, respectively) compare well with the literature [FW adaptation: 0.7x10-3 in Panouillères et al (2012a); BW adaptation: -8.5 x10-3, -0.69 x10-3, -1.4x10-3 and -0.52x10-3 in Gerardin et al (2012), Blurton et al (2012), Panouillères et al (2012a) and Guillaume et al (2018), respectively]. Together, these behavioral findings suggest that despite their limited duration (31.2 s) and number of trials (16), BW and FW blocks could elicit reliable and reproducible adaptation of reactive saccades.

4.3. Adaptation + Error

One of the challenging aims of this study was to tease apart the saccadic adaptation mechanisms contributing specifically to the adaptive changes of saccades from those involved in the processing of saccadic errors which lead to such oculomotor changes. Most previous neuroimaging studies of saccadic adaptation contrasted blocks of saccades toward double-step targets (second step during the saccade) vs. blocks of saccades toward single-step targets (PET: Desmurget et al., 1998, 2000), or blocks of saccades toward double-step targets with a short vs. long post-saccadic delay of the second step (fMRI: Gerardin et al., 2012; Blurton et al., 2012). This approach of contrasting between 'adaptation' and 'control' blocks (corresponding to our 'BW' / 'FW' versus 'STA' blocks) could not exclude the participation of mechanisms of error processing and of corrective saccades generation in the sources of metabolic activation. The same limitation applies to the only existing MEG study of saccadic adaptation to date (Nicolas et al., 2019b) which reported an increase

of gamma-band activity (GBA) during backward adaptation of leftward reactive saccades in a large cortical region of the right hemisphere including the posterior parietal cortex (PPC). Indeed, this electrophysiological signature of increased cortical excitability (Jensen & Mazaheri, 2010; Martinovic & Busch, 2011) could as well be related to the change of saccade error signal during adaptation exposure, a possibility consistent with the previously proposed role of GBA in saccade goal encoding by the PPC (Medendorp et al., 2007; Van Der Werf et al., 2008). Overall, these studies together clearly point at a contribution of cortical networks to saccadic adaptation, but could not attribute any specific role to these networks in the oculomotor plasticity component versus error signals processing component of adaptation.

4.4. Error

Guillaume et al. (2018) used an event-related fMRI approach to identify the activity specifically related to the size of the post-saccadic error induced by a backward target jump during leftward saccades, revealing activation in the cerebellum (left lobule V and right lobule VI), in the superior precentral sulcus and the paracentral sulcus of the right cerebral hemisphere (which they identified as FEF and SEF, respectively), and in the intraparietal and parieto-occipital sulci, the precuneus and the supramarginal gyrus of the left hemisphere. These frontal and parietal clusters were found in the ipsilateral or contralateral hemisphere, respectively, relative to the direction of post-saccadic visual error.

Our own results collected in a paradigm of backward target jump during rightward saccades disclosed the involvement of the left inferior cerebellum and right superior cerebellum, the cingulate cortex and in the following areas of the left hemisphere: the occipital cortex, precuneus and parietal cortex (SPL and PEF). Disclosure of a cerebellar involvement agrees with several previous studies in humans (van Broekhoven et al., 2009; Liem et al., 2012; Guillaume et al., 2018) and in non-human primates (Herzfeld et al., 2018). More specifically, given the size of errors relative to saccade size (4°/16° or 5°/20°) in the present study, the left inferior and right superior hemispheric areas we disclosed correspond to the lobules VIII/IX and lobule VI found by Liem et al. (2012) for their 'large errors' (5°/20°); in addition, the more medial areas -including vermis- reported by Guillaume et al. (2018) for their 3° errors (relative to a 16° saccade size) were also reported by Liem et al. for their 'small errors' (1.5°/20°). The presently demonstrated recruitment of inferior cerebellar areas in error signals processing is also consistent with the possibility that activation of lobules VIIb–VIIIa reported by Gerardin et al. (2012) during saccade adaptation exposure might in fact have been related to the processing of post-saccadic errors. Importantly, the recruitment of cerebral cortical areas in saccade error encoding also confirms and extends previous findings. While the left precuneus and the left

parietal cortex (SPL and PEF) were first reported by Guillaume et al. (2018), the involvement of the middle cingulate cortex (MCC) is a quite novel finding in the context of saccadic adaptation, however fully consistent with its well-described role in error detection or in performance monitoring in the more general context of decision making and cognitive control (see e.g. O'Connell et al., 2007; Nieuwenhuis et al., 2001; Endrass et al., 2005; Rupp et al., 2011; and for meta-analyses Beckmann et al., 2009 and Garrison et al., 2013). Also, our results echo the proposal of a hierarchical processing of errors in the cerebral cortex according to which the parietal cortex evaluates low-level errors associated with the processing of visual target information (e.g., target position perturbation) and the cingulate cortex encodes high-level errors that occur when participants fail to meet the task goal (Krigolson & Holroyd, 2007). Further, our data regarding the PPC also fit with recent electrophysiological data in non-human primate which suggest that the lateral intraparietal area (LIP) encodes saccadic motor error (Zhou et al., 2016; Munuera & Duhamel, 2020). Munuera and Duhamel (2020) notably reported a subpopulation of LIP neurons which encode errors specifically after contralateral primary saccades regardless of the error direction. This last observation matches with the present finding that parietal cortical areas (SPL, PEF, precuneus) recruited in relation to post-saccadic errors were all in the left hemisphere, i.e. contralateral to the primary saccades. Finally, the precuneus and, to a lesser extent, the posterior intraparietal sulcus and anterior portions of the occipital cortex, have been shown to encode eye position (Williams & Smith, 2010) which might contribute to the computation of a saccadic error information. Overall, our neuroimaging findings bring additional evidence based on oculomotor behavior in human to the above literature indicating that the cerebral network devoted to action monitoring and error detection involves both the cingulate cortex and the PPC.

4.5. Adaptation

Our approach also allowed us to identify the neural substrates of the plastic component of adaptation. Noteworthy, none of the 34 tested ROIs could discriminate between high and low saccadic amplitudes, suggesting that the areas discussed below are likely linked to the adaptation state itself and not to the resulting changes of saccade size (Tse et al., 2010).

Our results confirm the involvement of the MT/V5 complex found by Gerardin et al. (2012). However, whereas these authors reported only the hemisphere contralateral to saccade direction (right hemisphere for leftward saccades), we found a bilateral recruitment of this complex. The fact that Gerardin et al's study and ours used two different strategies to elicit saccadic adaptation (post-saccadic or intra-saccadic target steps, respectively) argues for a more direct implication in

oculomotor plasticity of area MT/V5 than a mere responsiveness to visual motion stimuli (Zeki et al., 1991; Watson et al., 1993). In contrast for the FEF, an opposite difference between the two studies was found, FEF being revealed in both hemispheres by Gerardin et al. (2012) but only in the ipsilateral (right) hemisphere in the present study. Such differences of recruitment patterns for MT/V5 and FEF could be related to the fact that we combined here the two directions of adaptation whereas Gerardin et al (2012) studied only backward adaptation. The unilateral involvement of the FEF reported here parallels that of the pallidum (recruited solely in the right hemisphere), which could be related to the known anatomical and functional relationships of the basal ganglia with the ipsilateral frontal cortex, including the FEF. This pallidal involvement is an original finding signalling a possible role of the basal ganglia in saccade adaptation. Consistent with this hypothesis, two clinical studies have reported that Parkinson's disease patients exhibit a decreased amount, although without complete loss, of reactive saccades adaptation (MacAskill et al., 2002; Abouaf et al., 2012). It is also well established that the basal ganglia system plays a critical role in various forms of behavioral plasticity (see for reviews Doyon & Benali, 2005; Lee et al., 2012; Hélie et al., 2015; Carland et al., 2019) with, in particular, a role of the pallidum in encoding prediction errors during unsupervised reinforcement learning (Garrison et al., 2013). While saccadic adaptation is a supervised motor learning process, similar plastic changes of saccades can be induced by unsupervised reinforcement learning (Madelain et al., 2011). Further, adaptation can be boosted when the saccadic targets consist of social stimuli, which most likely increase reinforcing signals (Meermeier et al., 2017). Together, these reports suggest that saccadic adaptation could to some extent rely on reinforcement learning, which could in turn account for the recruitment of the basal ganglia. This suggestion echoes recent anatomical data showing that the cerebellar-cortical loops and the basal ganglia cortical loops are more intertwined than previously thought (Bostan & Strick, 2018).

Do cortical areas disclosed in the present study causally contribute to the computation and the transmission to the brainstem saccadic generator of corrective oculomotor commands subtending adaptive changes of saccade metrics? Or does their neural activity reflect the known consequences of saccadic adaptation on spatial localization performance (Masselink & Lappe, 2021; Collins et al., 2009; Cheviet et al., 2022) and visuo-attentional abilities (Habchi et al., 2015; Nicolas et al., 2019a,b, 2020)? The contribution of the FEF -and associated pallidum- may be part of the former type, due to the rather direct FEF connection with the brainstem and superior colliculus saccadic circuitry. Alternatively, one can note that the FEF area involved in the present study more closely corresponds to the medial FEF than to the lateral FEF reported in previous neuroimaging works (reviewed in Cieslik et al 2016; see Müri 2006 for another review discussing a similar dissociation between a superior FEF and an inferior FEF). These two review papers propose that the medial -or superior- FEF is more

involved in cognitive control than in direct oculomotor control as opposed to the lateral -or inferior- FEF, which would be consistent with the perceptual effects of saccadic adaptation (Zimmerman et al., 2016), including the effect of adaptation we previously disclosed on visual attention (Habchi et al 2015; Nicolas et al 2019a,b, 2020) and on visuo-spatial localization (Cheviet et al 2022). But the distinction between these two non-exclusive hypotheses awaits further studies based on a causal approach, such as measuring the effects of neurostimulation or of patients' lesion on adaptation levels. For the other cortical areas revealed here (occipital visual cortex, MT/MST, infero-temporal cortex) and even possibly the FEF, we would rather favour the latter type of functional relationship to saccadic adaptation, as these areas are all related to visuo-spatial processes underlying localization or attention performance. Indeed, the occipital visual cortex and MT/MST are targeted by the superior colliculus through a tecto-thalamo-cortical pathway (Wurtz et al., 2011) thought to provide an oculomotor corollary discharge subtending accurate trans-saccadic spatial localization (Sommer & Wurtz, 2008; Thakkar et al., 2017; Cheviet et al., 2021). It has also been proposed that a cerebello-thalamo-cortical pathway supplies the cerebral cortex with a saccadic error signal between the predicted and actual consequences of the eye displacement (Peterburs & Desmond, 2016). And during saccadic adaptation, a cerebellar influence onto the cerebral cortex has further been suggested based on the behavioral performance of thalamic patients (Gaymard et al., 1994) and of patients with cerebellar neurodegenerative disease (Cheviet et al., 2022). The results of this last study were interpreted as the cerebellar pathology leading to inappropriate adaptation-related updating of the cerebral representations of both the saccade visual target and, to a lesser extent, the saccadic movement (efference copy). Taken together, we suggest that the cortical visual network delineated here encodes cerebellar-derived, adaptation-updated, information about the desired and actual saccade metric. Note that the presently demonstrated involvement of the cerebellum in error encoding but not in saccadic plasticity itself could be due to the fact that the oculomotor vermis previously reported (Desmurget et al., 2000; Guillaume et al., 2018) was not part of the ROIs tested here.

4.6. Direction of adaptation/error

Previous neuroimaging studies of saccadic adaptation have mainly focused on backward adaptation. In their PET study, Desmurget et al. (1998, 2000) did test forward adaptation and reported activation in the cerebellar vermis but not in FEF and SC, a pattern similar to what they found when considering forward and backward adaptation together. However they did not consider the backward condition separately and thus one cannot assess the specificity of this cerebellar activation relative to the direction of adaptation. Further, in their study of saccadic error processing,

Liem et al. (2012) disclosed an involvement of the vermal areas and lobule VI for forward errors and of the lobules VIII/IX for backward errors.

Here, we aimed through our last MVPA (MVPA-2: forward vs. backward directions) at identifying within the neural substrates of adaptation and/or of error signals processing of rightward saccades those specifically evoked in the backward or in the forward condition. Complementing Liem et al. (2012)'s findings, our results revealed five non-cerebellar areas. The forward condition was associated to the right pallidum and two cortical areas in the left hemisphere (occipital cortex and area MT/MST). Interestingly the two homologous cortical areas in the right hemisphere were related to the backward direction. Since all tested saccades were directed to the right, these occipital cortex and MT/MST areas were in the contralateral hemisphere relative to the adapted (backward or forward) direction whereas the pallidum was found in the ipsilateral hemisphere (relative to the forward direction). Further, according to our MVPA procedure designed to discriminate between the plastic and error processing components of saccadic adaptation, the occipital cortex encodes the contralateral saccadic errors, the MT/MST area relates to contralateral adaptive saccade changes, and the right pallidum relates to ipsilateral adaptive saccade change (the failure to identify the left pallidum could be caused by an insufficient sensitivity). Noteworthy, even though the right FEF was not highlighted by our backward vs. forward discrimination analysis, its involvement in adaptive changes could be predicted, based on the basal ganglia cortical loops, to follow the same directional specificity as that of the right pallidum.

4.7. Conclusions

Taken together, the present data add to the growing literature supporting a role of the cerebral cortex in saccadic adaptation and error processing through feedback and feed-forward relationships with the cerebellum. Such rather complex architecture of sensorimotor plasticity and of its impact on cognition provides new building blocks for future conceptual models.

5. Acknowledgements:

We thank the CERMEP Primage MRI engineers Franck Lamberton, and Danielle Ibarrola for invaluable help in data collection, and Frédéric Volland for his help in the set-up. We thank Dr. Alain Guillaume for useful comments on a previous version of this manuscript. We also thank all the volunteers who took part in the study.

Funding: This research was funded by the 'Agence Nationale de la Recherche' (ANR-15-CE37-0014-01 to DP). JN and AC were supported by a doctoral fellowship from 'Fondation de France'.

6. Data and code availability statement

The raw data are available as Nifti files (MRI) and EyeLink EDF files (eye movements) in an OSF project (https://osf.io/9q4rp/?view_only=20d21199ecf8425abda1f8cfe533a788). The codes of the experimental procedure, developed in the ExperimentBuilder environment 2.1.512 (SR Research) are also included as an ExperimentBuilder project in the same OSF project. Analyses of eye movements have been performed in the Matlab environment (R2015b) and all pre-processing and analyses of the fMRI data have been performed in the freely available SPM12 software.

7. References:

Abouaf L, Panouillères M, Thobois S, Majerova V, Vighetto A, Pélisson D, Tilikete C. 2012. Saccadic system plasticity mechanisms in Parkinson disease patients. J. Fr. Ophtalmol. 35(4):242-50

Alahyane N, Fonteille V, Urquizar C, Salemme R, Nighoghossian N, Pelisson D, Tilikete C. 2008. Separate neural substrates in the human cerebellum for sensory-motor adaptation of reactive and of scanning voluntary saccades. The Cerebellum. 7(4):595–601. https://doi.org/10.1007/s12311-008-0065-5.

Anderson TJ, Jenkins IH, Brooks DJ, Hawken MB, Frackowiak RS, Kennard C. 1994. Cortical control of saccades and fixation in man. A PET study. Brain, 117(Pt 5):1073–1084. [PubMed: 7953589]

Avila E, van der Geest JN, Kengne Kamga S, Verhage MC, Donchin O, Frens MA. 2015. Cerebellar transcranial direct current stimulation effects on saccade adaptation. Neural Plast. 2015:1–9. https://doi.org/10.1155/2015/968970.

Bahcall DO, Kowler E. 1999. Illusory shifts in visual direction accompany adaptation of saccadic eye movements. Nature. 400(6747): 864–866. https://doi.org/10.1038/23693.

Barash S, Melikyan A, Sivakov A, Zhang M, Glickstein M, Thier P. 1999. Saccadic dysmetria and adaptation after lesions of the cerebellar cortex. J Neurosci. 19(24):10931–10939. https://doi.org/10.1523/jneurosci.19-24-10931.1999

Beckmann M, Johansen-Berg H, Rushworth MF. 2009. Connectivity-based parcellation of human cingulate cortex and its relation to functional specialization. The Journal of Neuroscience, 29:1175–1190. [PubMed: 19176826]

Bender J, Tark K-J, Reuter B, Kathmann N, Curtis CE. 2013. Differential roles of the frontal and parietal cortices in the control of saccades. Brain and Cognition, 83: 1–9

Bey, K., Lippold, J.V., Aslan, B., Hurlemann, R., Ettinger, U. Effects of lorazepam on prosaccades and saccadic adaptation. J Psychopharmacol, 2021, Vol. 35(1) 91–99

Blurton SP, Raabe M, Greenlee MW. 2012. Differential cortical activation during saccadic adaptation. J Neurophysiol. 107(6):1738–1747. https://doi.org/10.1152/jn.00682.2011.

Bostan, A.C., and Strick, P.L. 2018. The basal ganglia and the cerebellum: nodes in an integrated network. Nat Rev Neurosci. 19(6): 338–350. doi:10.1038/s41583-018-0002-7.

Bridgeman, B., Hendry, D., & Stark, L. 1975. Failure to detect displacement of the visual world during saccadic eye movements. Vision Research, 15(6), 719‑ 722. https://doi.org/10.1016/0042-6989(75)90290-4

Brett, M., Anton, J.L., Valabregue, R., Poline, J.B. 2002. Region of interest analysis using an SPM toolbox Abstract presented at the 8th International Conference on Functional Mapping of the Human Brain, June 2-6, Sendai, Japan.

Carland MA, Thura D, Cisek P. 2019. The Urge to Decide and Act: Implications for Brain Function and Dysfunction. Neuroscientist. 25(5):491-511. doi: 10.1177/1073858419841553.

Cheviet, A., Pisella, L., and Pélisson, D. 2021. The posterior parietal cortex processes visuo-spatial and extra-retinal information for saccadic remapping: a case study. Cortex, 139: 134-151

Cheviet, A., Masselink, J., Koun, E., Salemme, R., Lappe, M., Froment-Tilikete, C., Pélisson, D. 2022. Cerebellar signals drive motor adjustments and visual perceptual changes during size adaptation of reactive saccades. Cerebral Cortex, doi: 10.1093/cercor/bhab455

Choi K-D, Kim H-J, Cho BM, Kim JS. 2008. Saccadic adaptation in lateral medullary and cerebellar infarction. Exp Brain Res. 188(3): 475–482. https://doi.org/10.1007/s00221-008-1375-z.

Cieslik, E.C., Seidlera, I., Laird, A.R., Foxe, P.T., and Eickhoff, S.B. 2016. Different involvement of subregions within dorsal premotor and medial frontal cortex for pro- and antisaccades. Neurosci Biobehav Rev. 68: 256–269. doi:10.1016/j.neubiorev.2016.05.012.

Coiner B, Pan H, Bennett ML, Bodien YG, Iyer S, O'Neil-Pirozzi TM, Leung L, Giacino JT, Stern E. 2019. Functional neuroanatomy of the human eye movement network: a review and atlas. Brain Struct Funct. 224(8):2603-2617. doi: 10.1007/s00429-019-01932-7. Epub 2019 Aug 12.

Collins, T. & Doré-Mazars, K. 2006. Eye movement signals infuence perception: Evidence from the adaptation of reactive and volitional saccades. Vision Res. 46, 3659–3673.

Collins T, Rolfs M, Deubel H, Cavanagh P. 2009. Post-saccadic location judgments reveal remapping of saccade targets to non-foveal locations. J Vis. 9(5):29.1–29.9. https://doi.org/10.1167/9.5.29.

Collins T, Heed T, Röder B. 2010. Eye-movement-driven changes in the perception of auditory space. Atten Percept Psychophys. 72(3): 736–746. https://doi.org/10.3758/app.72.3.736.

Cotti J, Guillaume A, Alahyane N, Pelisson D, Vercher J-L. 2007. Adaptation of voluntary saccades, but not of reactive saccades, transfers to hand pointing movements. J Neurophysiol. 98(2):602–612. https://doi.org/10.1152/jn.00293.2007.

Curtis CE, Connolly JD. 2008. Saccade preparation signals in the human frontal and parietal cortices. J Neurophysiol 99: 133–145, doi:10.1152/jn. 00899.2007.

Desmurget M, Pélisson D, Grethe JS, Alexander GE, Urquizar C, Prablanc C, Grafton ST. 2000. Functional adaptation of reactive saccades in humans: a PET study. Exp Brain Res. 132(2):243–259. https://doi.org/10.1007/s002210000342.

Desmurget M, Pélisson D, Urquizar C, Prablanc C, Alexander GE, Grafton ST. 1998. Functional anatomy of saccadic adaptation in humans. Nat Neurosci. 1(6):524–528. https://doi.org/10.1038/2241.

Domagalik, A. Beldzik, E. Fafrowicz, M., Oginska, H., Marek, T. 2012. Neural networks related to pro-saccades and anti-saccades revealed by independent component analysis, NeuroImage 62 1325–1333, http://dx.doi.org/10.1016/j.neuroimage.2012.06.006.

Doré-Mazars, K. & Collins, T. 2005. Saccadic adaptation shifs the pre-saccadic attention focus. Exp. Brain Res. 162, 537–542

Doyon J & Benali H. 2005. Reorganization and plasticity in the adult brain during learning of motor skills. Curr. Opin. Neurobiol. 15, 161–167.

Endrass, T., Franke, C. & Kathmann, N. 2005. Error awareness in a saccade countermanding task. J. Psychophsiol., 19, 275–280.

Ethier V, Zee DS, Shadmehr R. 2008. Changes in control of saccades during gain adaptation. J Neurosci. 28(51):13929–13937. https://doi.org/10.1523/jneurosci.3470-08.2008.

Gaymard, B., Rivaud, S., & Pierrot-Deseilligny, C. 1994. Impairment of extra-retinal eye position signals after central thalamic lesions in humans. Experimental Brain Research, 102(1). https://doi.org/10.1007/bf00232433

Gaymard B, Rivaud-Péchoux S, Yelnik J, Pidoux B, Ploner CJ. 2001. Involvement of the cerebellar thalamus in human saccade adaptation. Eur J Neurosci. 14(3):554–560. https://doi.org/10.1046/j.0953-816x.2001.01669.x.

Garrison, J., Erdeniz, B., Done, J. 2013. Prediction error in reinforcement learning: a meta-analysis of neuroimaging studies. Neurosci Biobehav Rev. 37(7):1297-310. doi: 10.1016/j.neubiorev.2013.03.023. Epub 2013 Apr 6.

Gerardin P, Miquée A, Urquizar C, Pélisson D. 2012. Functional activation of the cerebral cortex related to sensorimotor adaptation of reactive and voluntary saccades. Neuroimage. 61(4):1100–1112. https://doi.org/10.1016/j.neuroimage.2012.03.037

Golla H, Tziridis K, Haarmeier T, Catz N, Barash S, Thier P. 2008. Reduced saccadic resilience and impaired saccadic adaptation due to cerebellar disease. Eur J Neurosci. 27(1):132–144. https://doi.org/10.1111/j.1460-9568.2007.05996.x.

Gray MJ, Blangero A, Herman JP, Wallman J, Harwood MR. 2014. Adaptation of naturally paced saccades. J Neurophysiol. 111(11):2343-54. doi: 10.1152/jn.00905.2013. Epub 2014 Mar 12.

Gremmler S, Bosco A, Fattori P, Lappe M. 2014. Saccadic adaptation shapes visual space in macaques. J Neurophysiol. 111(9):1846-51. doi: 10.1152/jn.00709.2013. Epub 2014 Feb 12.

Grosbras MH, Laird AR, Paus T. 2005. Cortical regions involved in eye movements, shifts of attention, and gaze perception. Hum Brain Mapp 25: 140–154. doi:10.1002/hbm.20145.

Guillaume A, Fuller JR, Srimal R, Curtis CE. 2018. Cortico-cerebellar network involved in saccade adaptation. J Neurophysiol. 120(5): 2583–2594. https://doi.org/10.1152/jn.00392.2018.

Habchi, O., Rey, E., Mathieu, R., Urquizar, C., Farnè, A. and Pélisson, D. 2015. Deployment of spatial attention without moving the eyes is boosted by oculomotor adaptation, Frontiers in Human Neuroscience, 9:426.

Haynes, J.D., and Rees, G. 2006. Decoding mental states from brain activity in humans. Nature Reviews in Neuroscience, 7: 523-534.

Hélie, S., Ell, S.W., Ashby, F.G. 2015. Learning robust cortico-cortical associations with the basal ganglia: an integrative review. Cortex. 64:123-35. doi: 10.1016/j.cortex.2014.10.011. Epub 2014 Oct 27.

Hernandez, T. D., Levitan, C. A., Banks, M. S., and Schor, C. M. 2008. How does saccade adaptation affect visual perception? J. Vis. 8.3, 1–16. doi: 10.1167/8.8.3

Herweg, NA,Weber, B, Kasparbauer, A, Meyhöfer, I, Steffens, M, Smyrnis, N, Ettinger, U. 2014. Functional magnetic resonance imaging of sensorimotor transformations in saccades and antisaccades. NeuroImage 102 : 848–860

Herzfeld, D.J., Kojima, Y., Soetedjo, R., and Shadmehr, R. 2018. Encoding of error and learning to correct that error by the Purkinje cells of the cerebellum. Nat. Neurosci., 21, 736–743.

Iwamoto, Y., and Kaku, Y. 2010. Saccade adaptation as a model of learning in voluntary movements. Exp. Brain Res. 204, 145–162. doi: 10.1007/s00221-010-2314-3

Jenkinson N, Miall RC. 2010. Disruption of saccadic adaptation with repetitive transcranial magnetic stimulation of the posterior cerebellum in humans. The Cerebellum. 9(4):548–555. https://doi.org/10.1007/s12311-010-0193-6.

Jensen O, Mazaheri A. 2010. Shaping functional architecture by oscillatory alpha activity: gating by inhibition. Frontiers in Human Neuroscience, 4.

Khan AZ, Heinen SJ, McPeek RM. 2010. Attentional cueing at the saccade goal, not at the target location, facilitates saccades. J Neurosci. 30:5481–5488.

Klingenhoefer S, Bremmer F. 2011. Saccadic suppression of displacement in face of saccade adaptation. Vision Res. 51(8):881–889. https://doi.org/10.1016/j.visres.2010.12.006.

Krigolson, O.E., Holroyd, C.B. 2007. Hierarchical error processing: different errors, different systems. Brain Res. 1155:70-80.

Lee D, Seo H & Jung MW 2012. Neural basis of reinforcement learning and decision making. Annu. Rev. Neurosci. 35, 287–308

Liem E, Frens MA, Smits M, van der Geest JN. 2012. Cerebellar activation related to saccadic inaccuracies. The Cerebellum. 12(2): 224–235. https://doi.org/10.1007/s12311-012-0417-z.

Lynch JC, Tian JR. 2006. Cortico-cortical networks and cortico-subcortical loops for the higher control of eye movements. Prog Brain Res 151: 461–501. doi:10.1016/S0079-6123(05)51015-X.

MacAskill MR, Anderson TJ, Jones RD. 2002. Adaptive modification of saccade amplitude in Parkinson's disease. Brain. 125(Pt 7):1570-82. doi: 10.1093/brain/awf168.

Madelain L, Paeye C, Wallman J. 2011. Modification of saccadic gain by reinforcement. J Neurophysiol. 106(1):219-32. doi: 10.1152/jn.01094.2009. Epub 2011 Apr 27. PMID: 21525366

Martinovic, J., Busch, N.A. 2011. High frequency oscillations as a correlate of visual perception. Int J Psychophysiol. 79(1):32-8. doi: 10.1016/j.ijpsycho.2010.07.004. Epub 2010 Jul 21.

Masselink J, Lappe M. 2021. Visuomotor learning from postdictive motor error. Elife. 10:e64278. https://doi.org/10.7554/eLife.64278.

McDowell, J.E. Dyckman, K.A. Austin, B.P. Clementz, B.A. 2008. Neurophysiology and neuroanatomy of reflexive and volitional saccades: evidence from studies of humans, Brain Cogn. 68 :255–270, http://dx.doi.org/10.1016/j.bandc.2008.08.016.

McLaughlin, S. C. 1967. Parametric adjustment in saccadic eye movements. Percept. Psychophys. 2, 359–362. doi: 10.3758/bf03210071

Medendorp WP, Kramer GFI, Jensen O, Oostenveld R, Schoffelen J-M, Fries P. 2007. Oscillatory activity in human parietal and occipital cortex shows hemispheric lateralization and memory effects in a delayed double-step saccade task. Cereb Cortex. 17:2364–2374.

Meermeier A, Gremmler S, Richert K, Eckermann T, Lappe M. 2017. The reward of seeing: Different types of visual reward and their ability to modify oculomotor learning. J Vis. 17(12):11. doi: 10.1167/17.12.11.

Munoz DP, Everling S. 2004. Look away: the anti-saccade task and the voluntary control of eye movement. Nat Rev Neurosci; 5(3):218–228. [PubMed: 14976521]

Munuera, J., Duhamel, J.R. 2020. The role of the posterior parietal cortex in saccadic error processing. Brain Struct Funct. 225(2):763-784. doi: 10.1007/s00429-020-02034-5.

Müri, R.M. 2006. MRI and fMRI analysis of oculomotor function. Progress in Brain Research, Vol. 151, Chap 16: 503-526, Elsevier B.V.

Nicolas, J., Bidet-Caulet, A. and Pélisson, D. 2019a. Inducing oculomotor plasticity to disclose the functional link between voluntary saccades and endogenous attention, Scientific Reports, 9 :17770. doi: 10.1038/s41598-019-54256-1

Nicolas, J., Bompas, A., Bouet, R., Sillan, O., Koun, E., Urquizar, C., Farnè, A., Bidet-Caulet, A., Pélisson, D. 2019b. Saccadic adaptation impacts gamma band oscillations during an attentional capture task. Cerebral Cortex, 29 (9): 3606-3617 (doi: 10.1093/cercor/bhy241)

Nicolas, J., Bidet-Caulet, A. and Pélisson, D. 2020. Reactive saccade adaptation boosts orienting of visuospatial attention, Scientific Reports, 10: 13430. https://doi.org/10.1038/s41598-020-70120-z

Nieuwenhuis, S., Ridderinkhof, K.R., Blom, J., Band, G.P. & Kok, A. 2001. Error-related brain potentials are differentially related to awareness of response errors: evidence from an antisaccade task. Psychophysiology, 38, 752–760

O'Connell RG, Dockree PM, Bellgrove MA, Kelly SP, Hester R, Garavan H, Robertson IH, Foxe JJ. 2007. The role of cingulate cortex in the detection of errors with and without awareness: a high-density electrical mapping study. Eur J Neurosci. 25(8):2571-9. doi: 10.1111/j.1460-9568.2007.05477.x.

Oosterhof, N.N., Wiestler, T & Diedrichsen, J. 2010. A comparison of volume-based and surface-based multi-voxel pattern analysis. Neuroimage, 56 (2), 593-600.

Optican, L.M., Robinson, D.A., 1980. Cerebellar-dependent adaptive control of primate saccadic system. J. Neurophysiol. 44, 1058–1076.

Panouillères, M., Weiss, T., Urquizar, C., Salemme, R., Munoz, D.P., Pélisson, D. 2009. Behavioral evidence of separate adaptation mechanisms controlling saccade amplitude lengthening and shortening. J. Neurophysiol. 101: 1550–1559.

Panouillères M, Neggers SFW, Gutteling TP, Salemme R, Stigchel S, van der Geest JN, Frens MA, Pélisson D. 2012a. Transcranial magnetic stimulation and motor plasticity in human lateral cerebellum: dual effect on saccadic adaptation. Hum Brain Mapp. 33(7):1512–1525. https://doi.org/10.1002/hbm.21301.

Panouillères M, Salemme R, Urquizar C, Pelisson D. 2012b. Effect of saccadic adaptation on sequences of saccades. J Eye Mov Res. 5(1):1.

Panouillères, M., Alahyane, N., Urquizar, C., Salemme, R., Nighoghossian, N., Gaymard, B., Tilikete, C., Pélisson, D. 2013. Effects of structural and functional cerebellar lesions on sensorimotor adaptation of saccades. EBR, 231: 1-11.

Panouillères MTN, Joundi RA, Brittain J-S, Jenkinson N. 2015. Reversing motor adaptation deficits in the ageing brain using non-invasive stimulation. J Physiol. 593(16):3645–3655. https://doi.org/10.1113/jp270484.

Pélisson D, Alahyane N, Panouillères M, Tilikete C. 2010. Sensorimotor adaptation of saccadic eye movements. Neurosci Biobehav Rev. 34(8): 1103–1120. https://doi.org/10.1016/j.neubiorev.2009.12.010

Peterburs J, Desmond JE. 2016. The role of the human cerebellum in performance monitoring. Curr Opin Neurobiol. 40:38–44.

Petit, L., Zago, L., Mellet, E., Jobard, G., Crivello, F., Joliot, M., Mazoyer, B., Tzourio-Mazoyer, N. 2015. Strong Rightward Lateralization of the Dorsal Attentional Network in Left-Handers With Right Sighting-Eye: An Evolutionary Advantage. Human Brain Mapping, 36:1151–1164

Rupp, J. Dzemidzic, M. Blekher, T. Bragulat, V. West, J. Jackson, J. Hui, S., Wojcieszek, J. Saykin, A.J. Kareken, D., and Foroud T. 2011. Abnormal error-related antisaccade activation in premanifest and early manifest Huntington disease. Neuropsychology 25(3): 306–318. doi:10.1037/a0021873.

Schnier F, Zimmermann E, Lappe M. 2010. Adaptation and mislocalization fields for saccadic outward adaptation in humans. J Eye Mov Res. 3(3). https://doi.org/10.16910/jemr.3.3.4.

Schnier, F., and Lappe, M. 2011. Differences in intersaccadic adaptation transfer between inward and outward adaptation. J. Neurophysiol. 106, 1399–1410. doi: 10.1152/jn.00236.2011

Schnier F, Lappe M. 2012. Mislocalization of stationary and flashed bars after saccadic inward and outward adaptation of reactive saccades. J Neurophysiol. 107(11):3062–3070. https://doi.org/10.1152/jn.00877.2011.

Semmlow JL, Gauthier GM, Vercher J-L. 1989. Mechanisms of shortterm saccadic adaptation. J Exp Psychol Hum Percept Perform. 15(2): 249–258. https://doi.org/10.1037/0096-1523.15.2.249

Sommer MA, Wurtz RH. 2008. Brain circuits for the internal monitoring of movements. Annu Rev Neurosci. 31(1):317–338. https://doi.org/10.1146/annurev.neuro.31.060407.125627.

Souto D, Gegenfurtner KR, Schütz AC. 2016. Saccade adaptation and visual uncertainty. Front Hum Neurosci. 10. https://doi.org/10.3389/fnhum.2016.00227.

Steenrod SC, Phillips MH, Goldberg ME. 2013. The lateral intraparietal area codes the location of saccade targets and not the dimension of the saccades that will be made to acquire them. Journal of Neurophysiology 109:2596–2605.

Straube A, Deubel H. 1995. Rapid gain adaptation affects the dynamics of saccadic eye movements in humans. Vision Res. 35(23–24): 3451–3458. https://doi.org/10.1016/0042-6989(95)00076-q.

Straube, A., Fuchs, A.F., Usher, S., Robinson, F.R., 1997. Characteristics of saccadic gain adaptation in rhesus macaques. J. Neurophysiol. 77, 874–895.

Straube A, Deubel H, Ditterich J, Eggert T. 2001. Cerebellar lesions impair rapid saccade amplitude adaptation. Neurology. 57(11): 2105–2108. https://doi.org/10.1212/wnl.57.11.2105.

Srimal R, Diedrichsen J, Ryklin EB, Curtis CE. 2008. Obligatory adaptation of saccade gains. J Neurophysiol. 99(3):1554-8. doi: 10.1152/jn.01024.2007

Srivastava, A., Sharma, R., Goyal, V., Chaudhary, S., Sood, S.K., Kumaran, S.S. 2019. Saccadic Eye Movements in Young-Onset Parkinson's Disease - A BOLD fMRI Study. Neuroophthalmology, 44(2):89-99. doi: 10.1080/01658107.2019.1652656.

Takagi M, Zee DS, Tamargo RJ. 1998. Effects of lesions of the oculomotor vermis on eye movements in primate: saccades. J Neurophysiol. 80(4):1911–1931. https://doi.org/10.1152/jn.1998.80.4.1911

Thakkar KN, Diwadkar VA, Rolfs M. 2017. Oculomotor prediction: a window into the psychotic mind. Trends Cogn Sci. 21(5):344–356. https://doi.org/10.1016/j.tics.2017.02.001.

Tse PU, Baumgartner FJ, Greenlee MW. 2010. Event-related functional MRI of cortical activity evoked by microsaccades, small visually-guided saccades, and eyeblinks in human visual cortex. Neuroimage 49: 805–816. doi:10.1016/j.neuroimage.2009.07.052.

van Broekhoven PCA, Schraa-Tam CKL, van der Lugt A, Smits M, Frens MA, van der Geest JN. 2009. Cerebellar contributions to the processing of saccadic errors. Cerebellum; 8(3):403–15.

Van Der Werf J, Jensen O, Fries P, Medendorp WP. 2008. Gamma-band activity in human posterior parietal cortex encodes the motor goal during delayed prosaccades and antisaccades. J Neurosci. 28:8397–8405.

Watson JD, Myers R, Frackowiak RS, Hajnal JV, Woods RP, Mazziotta JC, Shipp S, Zeki S. 1993. Area V5 of the human brain: evidence from a combined study using positron emission tomography and magnetic resonance imaging. Cereb Cortex, 3(2):79-94. doi: 10.1093/cercor/3.2.79.

Williams, A.L., Smith, A.T. 2010. Representation of Eye Position in the Human Parietal Cortex. J Neurophysiol., 104: 2169–2177.

Wurtz RH, McAlonan K, Cavanaugh J, Berman RA. 2011. Thalamic pathways for active vision. Trends Cogn Sci. 15(4):177–184. https://doi.org/10.1016/j.tics.2011.02.004.

Xu-Wilson M, Chen-Harris H, Zee DS, Shadmehr R. 2009. Cerebellar contributions to adaptive control of saccades in humans. J Neurosci. 29(41):12930–12939. https://doi.org/10.1523/jneurosci.3115-09.2009.

Zeki S, Watson J, Lueck C, Friston KJ, Kennard C, Frackowiak R 1991. A direct demonstration of functional specialization in human visual cortex. J Neurosci 11(3):641–649

Zhou Y, Liu Y, Lu H, Wu S, Zhang M. 2016. Neuronal representation of saccadic error in macaque posterior parietal cortex (PPC). eLife. 5:e10912.

Zimmermann E, Lappe M. 2010. Motor signals in visual localization. J Vis. 10(6):2. https://doi.org/10.1167/10.6.2.

Zimmermann E, Lappe M. 2016. Visual space constructed by saccade motor maps. Front Hum Neurosci. 100. https://doi.org/10. 3389/fnhum.2016.00225.